Critical Reviews in Biotechnology

ISSN: (Print) (Online) Journal homepage: https://www.tandfonline.com/loi/ibty20

Biomedical applications of the peptide decorated gold nanoparticles

Akhilesh Rai & Lino Ferreira

To cite this article: Akhilesh Rai & Lino Ferreira (2021) Biomedical applications of the peptide decorated gold nanoparticles, Critical Reviews in Biotechnology, 41:2, 186-215, DOI: 10.1080/07388551.2020.1853031

To link to this article: https://doi.org/10.1080/07388551.2020.1853031

CRITICAL REVIEWS IN BIOTECHNOLOGY
2021, VOL. 41, NO. 2, 186–215
https://doi.org/10.1080/07388551.2020.1853031

Taylor & Francis
Taylor & Francis Group

REVIEW ARTICLE

Biomedical applications of the peptide decorated gold nanoparticles

Akhilesh Rai[a,b] and Lino Ferreira[a,b]

[a]Center for Neuroscience and Cell Biology, University of Coimbra, Coimbra, Portugal; [b]Faculty of Medicine, University of Coimbra, Coimbra, Portugal

ABSTRACT

Currently, peptide-nanoparticle (NP) conjugates have been demonstrated to be efficient and powerful tools for the treatment and the diagnosis of various diseases as well as in the bioimaging application. Several bioconjugation strategies have been adopted to formulate the peptide-NP conjugates. In this review, we discuss the exciting applications of peptide-gold (Au) NP conjugates in the area of drug delivery, targeting, cancer therapy, brain diseases, vaccines, immune modulation, biosensor, colorimetric detection of heavy metals, and bio-labeling *in vitro* and *in vivo* models. Within this framework, various approaches such as radiotherapy, photothermal therapy, photodynamic therapy and chemo-photothermal therapy have been demonstrated for the treatment of several diseases. Moreover, we highlight how the morphology, size, density of peptide and the protein corona influence the biological activity, biodistribution and biological fate of peptide-AuNP conjugates. In the end, we discuss the future outlook and the challenges being faced in the clinical translation of the peptide-AuNP conjugates. Overall, this review emphasizes that the peptide-AuNP conjugates might be used as potential theranostic agents for the treatment of life-threatening diseases in an economical fashion in the future.

ARTICLE HISTORY
Received 10 June 2020
Revised 17 September 2020
Accepted 9 November 2020

KEYWORDS
Peptide-NP conjugates; cellular internalization; cancer therapy; immune response; blood brain barrier; antimicrobial NPs; gene delivery; stealth NPs

Introduction

Nanotechnology-based approaches offer advanced tools for biomedical applications ranging from diagnostics, bioimaging, biodetection, biosensors, and the delivery of drugs/genes and antimicrobial molecules (Figure 1). In the last few decades, colloidal AuNPs have been extensively explored for the development of multifunctional theranostic tools due to their unique and size-dependent physicochemical properties [1–5]. Furthermore, AuNPs have been most preferably chosen for the various biomedical applications given that their easy surface functionalization, biocompatibility and their quantification in both *in vitro* and *in vivo* models [1,3,6,7]. The surface of AuNPs can be functionalized with the thiol, phosphine or amine moieties containing biomolecules, although the thiol-based conjugation is the most promising way to immobilize biomolecules [8]. The strategy to modify the surface of AuNPs with biomolecules is vital to their applications in the area of nanomedicine. Surface functionalization not only affects the physicochemical (monodispersity, stability, and biocompatibility) property of NPs but also provides multifunctional moieties to conjugate several biomolecules on the same AuNP [5]. Hence, the compositions, morphologies, and size of biomolecule-NP conjugates affects their nature of biological activity and applications.

Peptides are a small chain of two or more amino acids, which are linked with one another by their peptide bonds. Peptides have attracted considerable attention in biomedical areas due to their excellent biological properties, cheaper synthesis methods and the possibility of designing sequences based on their interactions with receptors using an *in silico* approach [9,10]. Peptides can be classified into two categories: (i) synthetic peptides identified using peptide library screening or phage display library approaches and (ii) the peptide sequences from natural proteins [11–13]. Currently, more than 150 peptides are under different phages of clinical trials, demonstrating their potential as potent drugs [14–16]. However, the main concerns with peptides include their lower binding ability to target *in vivo* models, protease degradation and the short half-lives in the circulating system, resulting in frequent administrations of peptides to maintain their *in vivo* efficacy [9,11,14]. In recent decades, researchers have identified that peptide-AuNP conjugates can address many of these intrinsic issues of peptides. The combination of AuNPs' specificity and peptide versatility

CONTACT Akhilesh Rai akhilesh.rai@uc.pt Faculty of Medicine, University of Coimbra, Coimbra, Portugal

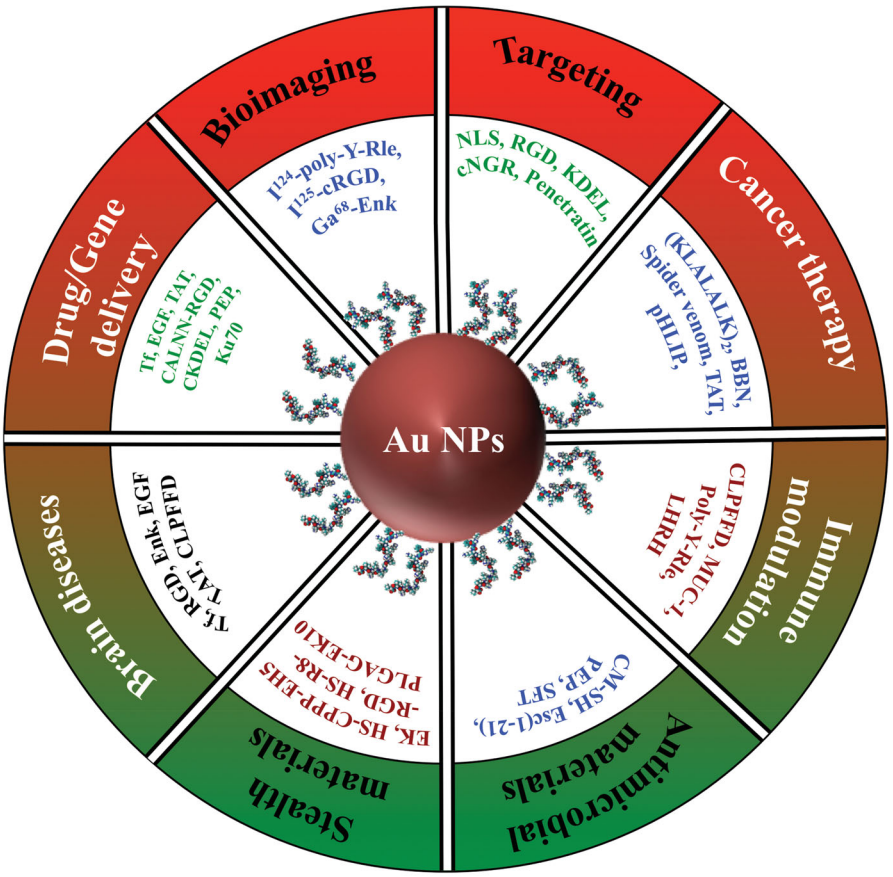

Figure 1. Schematic representation of peptide conjugated AuNPs explored in multiple applications.

improves the properties of peptide-NP conjugates several fold as compared to their counterparts. Therefore, designing and preparing multifunctional peptide-AuNP conjugates to treat several diseases has attracted huge attention in the last few years.

Molecular dynamics studies have revealed the contribution of molecular interactions of not only the individual amino acid residue of the peptide but also the whole peptide with Au surfaces [17,18]. These approaches have helped researchers to design custom-made peptides, which can strongly interact with AuNPs to produce well-defined nanostructures with precisely fine-tuned physicochemical and biological properties. For example, a single amino acid residue in peptides can be mutated to facilitate the specific orientation of peptides on the surface of NPs to program cellular uptake and to manipulate immune responses [19–21]. Importantly, a diverse range of peptide-AuNP conjugates have been developed for the various biomedical applications [22–26]. However, the development of peptide-AuNP conjugates using biocompatible and reproducible methods, which can help in personalized or general treatments of the most common diseases, is a key question in nanomedicine. Keeping in mind the desired applications, the specific peptide-AuNP conjugates could be produced on a large-scale without compromising their bioactivity. Multifunctionality of these peptide-AuNP conjugates offers great advantages over the bare peptides or NPs, including the enhanced delivery of hydrophobic drugs to improve pharmacokinetics, bioimaging and site-specific targeting to minimize systemic toxicity along with controlled drug release in response to stimuli such as pH, light, thermal, redox and enzyme-triggered strategies.

This review focuses on a comprehensive overview of the formulation of peptide-AuNP conjugates and their applications in biomedicine, biosensor, imaging and photothermal/photodynamic therapy (Figure 1). Although several reviews have been published on the subject of peptide/protein-NP conjugates [22–25,27,28], this review covers the vast extensive applications of peptide-AuNP conjugates, which have not been discussed previously in a single manuscript. This review exclusively highlights how different factors govern the bioactivity of peptide-AuNP conjugates and a single type of peptide-AuNP conjugates can be used for multiple applications. We have selected examples of AuNPs because AuNPs have been widely used for various biomedical applications. Therefore, this review will present detailed references in this area for both experts and

beginners. Additionally, we hope that this review will stimulate readers to select the suitable peptides for the desired applications or to promote innovations in the peptide-AuNP conjugate field in order to overcome obstacles that continue to prevent their clinical translations.

Advantage of peptide-AuNP conjugates

AuNPs are distinct from small molecules and bulk Au and therefore are widely used for the biomedical applications due to their unique physicochemical properties [7,29]. Peptide-AuNP conjugates offer multifunctional and enhanced biomedical properties over free peptides. The selectivity of the peptide-AuNP conjugates can be improved by fine-tuning the density or the orientation of conjugated peptides, which facilitates stronger interactions with the receptors of cells. Furthermore, the conjugation of multiple peptides and/or biological materials on AuNPs offers multiple functionalities such as a stimulus property, immune response, theranostics and drug delivery amongst others (Tables 1 and 2). Importantly, small drugs exhibit rapid clearance and poor pharmacokinetics, leading to low therapeutic effects *in* the animal models [30]. Additionally, there are issues with the administration of lesser water-insoluble or hydrophobic drugs [31]. The ability of peptide-NP conjugates to deliver hydrophobic or small drugs to the target sites makes them attractive agents to accelerate the process of drug discovery. Peptide-AuNP conjugates improve the solubility of drugs in aqueous solution, circulation time in blood, tissue targeting and their high levels of accumulation in the specific cells or tissues [13]. Additionally, the encapsulation of drugs in the peptide-NP conjugates avoids severe side effects by specifically targeting the desired cells and the sustained drug release inside them [13].

The benefits of peptide-NP conjugates have been extensively explored in the field of cancer imaging and therapy [32–34]. Despite the variety of drug-coated NPs being demonstrated for cancer therapy in the last few years, only a very small amount of the administered dose of NPs accumulates in solid tumors. Multifunctionalities of peptide-AuNP conjugates have been explored in terms of the delivery of cancer drugs to the target sites to reduce unwanted side effects, photothermal therapy (PTT), radiotherapy and the imaging of cancer cells *in* animal models [35] (Table 2). Indeed the peptide-AuNP conjugates have also been utilized for photoacoustic (PA), computed tomography (CT) and fluorescence imaging [36].

Colorimetric detection of biological and chemical materials, using the peptide-AuNP conjugates, is of great importance due to their high sensitivity, cost-effectiveness and a convenient way for detection. AuNPs aggregate in the presence of analytes, leading to the color change of NP solution from red to blue and consequently the shift of the SPR band due to interparticle surface plasmon coupling. The extent of color change depends on the concentration of analytes, facilitating the design of biosensors to detect biochemicals for the diagnostics and bioanalytical applications. Peptide-AuNP conjugates offer selectivity in which a specific biochemical can be detected from the pool of biochemicals in the range of picomolar concentrations [37].

Properties and applications of peptide-AuNP conjugates

Cellular uptake and drug delivery

Understanding the interactions of peptide-NP conjugates with cells or tissues are of uttermost importance to develop effective agents for therapy and imaging. The information related to how size, shape and functionality of NPs affects their cellular fate, which could help us to design the appropriate peptide-NP conjugates for specific applications. For instance, peptide engineering can modulate the endocytosis or exocytosis of peptide conjugated AuNPs [38]. The internalization efficiency of peptide conjugated NPs depends on several factors such as: amphipathicity, charge and guanidinium content in the peptides. The number and sequence of amino acid, especially the charged ones, controls the overall charge and secondary structure of peptides and therefore will significantly affect the internalization patterns of peptide conjugated NPs due to the variation in interactions with cell receptors or membranes. Importantly, the stability of peptide conjugated NPs in biological media depends on their surface charges, which influences the cellular internalization efficiency [21]. Readers will find several examples of how the peptide sequence modulates the cellular internalization efficiency of NPs in the below section.

Cellular internalization

Cell-penetrating peptides (CPPs) have widely been used for cellular internalization of AuNPs to deliver drugs and oligonucleotides. A new class of CPP called sweet arrow peptide (SAP, $(VRLPPP)_3$) is identified to be effective in cellular translocation without imposing cytotoxicity [39]. Transmission electron microscopy (TEM), confocal laser scanning microscopy (CLSM) and

Table 1. The sequence of peptides used in the preparation of peptide-AuNP conjugates and their applications.

Peptide sequence and name	Morphology of Au NPs	Conjugation chemistry	Applications	References
$CALN_2AGRK_2R_2QR_3$ (TAT)	Spherical	CALNN	Enhanced intracellular delivery	[41,42]
$VTPH_2VLVDEYTGEWVDSQFK$ (VG21)	Spherical	EDC chemistry	Enhanced translocation efficiency	[43,44]
$CALN_2GRQIKIWFQNR_2MKWK_2$ (Penetratin)	Spherical	CALNN	Endosomal and nuclei uptake	[42]
$YGRK_2R_2QR_3$ (TAT)	Spherical	EDC/NHS	Nuclear targeting	[46]
$CALN_2$ (pentapeptide), $CG_2RK_2R_2QR_3AP$ (NLS), $CK_6G_2RGDMFG$ (RGD contains peptide)	Spherical	Direct	Intracellular and nuclear delivery	[49]
GDIMGEWGNEIFGAIAGFLGC (HA2), $KYGR_3QR_2K_2RGC$ (TAT)	Rod	SPDP	Enhanced cellular and nuclear localization, Cancer therapy	[50]
CKDEL	Spherical	Thiol-Au	Endoplasmic reticulum targeting	[53]
Ac-$WGR_2VR_3IR_2P_9G_2K$ (CPP)	Spherical	EDC/NHS	Cellular internalization	[54]
$(KLALALK)_2$, (PAP)	Spherical	Thio-Au	Cancer therapy	[62,63]
WKRAKLAK	Spherical, rod	Thio-Au	Cancer therapy	[64]
LTVSPWY, $WNLPWY_2SVSPT$, RGDPAYQGRFL, WXEAAYQRFL, GNHWAVGHL (THPs)	Spherical	NHS-PEG_8-Maleimide	Cancer therapy	[65]
cRGD-^{177}Lu	Spherical	Thiol-Au	Radio and cancer therapy	[67]
$ACEQNPIYWARYADWLFT_2PL_4DLAL_2VDADET$ (pHLIP)	Spherical	Thiol-Au	X-ray irradiation for cancer therapy	[69,70]
Cyclic-CYG_2CNGRC (c-NGR)	Spherical, Rod	Thiol-Au	PA/X-ray-CT/photothermal imaging of cancer	[72]
$KYFP_2LALYNPTEYFY$ (P75 peptide)	Nanotriangles	Thiol-Au	CT/PA imaging of cancer	[76]
Y_9C (poly-Y-Rle)	Spherical	Thiol-Au	PET7CT imaging of tumor	[77]
$TSFAEYWNL_2SP$ and CRGDK	Spherical	EDC/NHS and Thiol-Au	Tumor treatment	[78]
RGDRGDRGDRGDPGC and $CGGGPK_3RKVG_2$	Spherical	Thiol-Au	Cancer therapy	[80]
$YSAYPDSVPM_2S$ (YSA peptide)	Spherical	Electrostatic interactions	Cancer therapy	[81]
$S_2G_3QWAVGHLM$ (BBN)	Rod	Thiol-Au	Cancer therapy	[82–84]
VSNKYFSNIHW (uPAR)	Spherical	PEG Spacer with thiol	Cancer therapy	[85,86]
$MDDRWPLEYTD_2TYEIPW$	Spherical	EDC/NHS	Cancer therapy	[90]
$KATWLP_2R$	Rod	EDC/sulfo-NHS	Tumor angiogenesis and hyperthermia	[99,99]
YSA	Nanoshell	OPSS-PEG-NHS	Hyperthermic killing of PC3 cells	[81, 100]
IAGLATPGWSHWLAL	Spherical	EDC/NHS	Hyperthermic killing of PC3 cells	[108]
Tf ($THRP_2MWSPVWP$)-$CLPF_2D$	Spherical	Thiol-Au	Brain delivery	[118]
KAPETAL	Spherical	Thiol-Au	Brain targeting	[119]
$THRP_2MWSPVWPC$ (Tf)	Spherical and NRs	Amine-PEG-maleimide	Brain targeting	[121]
GRGDG-NH_2	Spherical	Amine-Au	Brain glioma and imaging	[123,124]
YG_2FL and $G_3YTGFLS$-O-β-glucoside (Glycopep)	Spherical	Thiol-Au	BBB transcytosis and imaging	[125]
$CLPF_2D$	Spherical, nanostar and rod	Thiol-Au	Alzheimer's diseases	[131–133,135,137]
$CLPF_2D$, $CDLPF_2$, $CLPDF_2$ and $C(VRLPPP)_3$, $CLPA_2D$	Spherical	Thiol-Au	Immune response	[20,138]
Y_9C (poly-Y-Rle)	Spherical	Thiol-Au	Cancer immunotherapy	[77]
$RPGSV_3QLTLAFREGTIN$ VHDVETQFNQYKTEA$_2$SRYNLTISDVS (MUC-1 peptide)	Spherical	Thiol-Au	Breast cancer therapy, vaccine development	[142–145]
CS_2CS_2CPLSK	Spherical	Thiol-Au	Immune response	[146]
$SI_2NFEKLC$ ($OVA_{257-264}$ peptide)	Spherical	Thiol-Au	Therapy for liver infection	[150]
$ISQAVHA_2HAEINEAGR$ ($OVA_{329-339}$ peptide)	Spherical	Thiol-Au	Bacterial infection	[151]
$KWKLFK_2IGAVLKVLC$ (CM-SH)	Spherical	Thiol-Au	Bacterial infection	[166]
$GIFSKLAGK_2IKNL_2ISGLKG$ (Esc_{1-21})	Spherical	EDC/NHS	*P. aeruginosa* infection	[167]

Table 2. Peptide-NP conjugates in the drug delivery applications.

Peptide sequence	Drugs	Morphology of NPs	Applications	References
CRGDK	Pt(IV)	Spherical	Treatment of prostate cancer	[79]
$CALN_2K_3RGD$	DOX	Spherical	Cancer therapy	[93]
Derivative of $CALN_2$	DOX and Mitoxantrone	Spherical	Cancer therapy	[95]
$HSTPS_2P$	chlorambucil (Chlor), melphalan (Melph) or bendamustine (Bend)	Spherical	Cancer therapy	[96]
CKDEL	NADPH oxidase isoform 4(Nox4) siRNA	Spherical	Treatment of muscle disease	[154]
$VHSPNK_2G_2SKGC$	anti-athero-miRNAs (miR-712)	Spherical	Treatment of Atherosclerosis	[155]
cRGD installed poly(ethylene glycol)-block-poly(l-lysine)	siRNA	Spherical	Tumor therapy	[159,160]
$C_2YGR_3QR_2K_2RGR_3$	Antisense oligonucleotide (ASO) and pDNA-Mi221	Spherical	Skin cancer therapy	[161,162]
$CYSL_{50}$	Short ssDNA and siRNA	Nanoshell	Cancer therapy	[163]
HS-CP_3-EK5-RGD and HS-R8-PLGLAG-EK10	5-Aminolevulinic acid (ALA)	Spherical	Cancer therapy	[177,178]
YHWYGYTPQNVI (EGF receptor peptide) and HAIYPRH (Tf peptide)	Pc4 drug	Spherical	Brain tumor	[126,127]
$YGRK_2R_2QR_3$ (TAT)	DOX	Spherical	Brain tumor therapy and imaging	[128,129]

transmission X-ray microscopy (TXM) reveled effective intracellular delivery of SAP conjugated AuNPs in HeLa cells in comparison to bare NPs [40]. Brust's group observed an unusual trend of TAT conjugated AuNPs inside HeLa cells. TAT-AuNPs initially accumulated in the cytosol, nucleus and mitochondria. However, later AuNPs translocated in densely filled vesicles, possibly due to direct membrane transfer within the subcellular organelles of cells [41]. On the other hand, CALNN elongated TAT peptide promotes predominantly the accumulation of AuNPs in endosomes [42]. VG-21 (Figure 2) and penetratin peptides derived from vesicular stomatitis virus and Drosophila antennapedia homodomain (Antp) respectively have been described as CPPs to efficiently deliver AuNPs into cytosols of HEp-2, HeLa, Vero, Cos-7 and bovine immortalized endothelial cells [43,44]. VG21-AuNPs reduced the expression of the stress response gene in HEp-2 cells [44]. On the contrary, the combination of TAT and the penetratin peptide improved the accumulation of AuNPs in cytosols of HeLa cells in addition to endosomal uptake [42] (Table 1). Furthermore, the cellular internalization efficiency of AuNPs can be increased when the surface of NPs functionalizes with the CPP containing a lipid moiety. The lipid moiety helps better penetration of NPs inside the cellular membrane. Myristoylated hendeca-D-arginine peptide (MLP) conjugation AuNPs promoted the elevated cellular internalization, low cytotoxicity and enhanced metabolic stability as compared to the acetylated hendeca-D-arginine peptide (ALP) conjugated NPs [45].

Nuclear targeting

Several strategies have been developed to achieve the localization of peptide-AuNP conjugates inside the nucleus to deliver RNA/DNA and drugs because there are several barriers inside cells that must be crossed by NPs before reaching the nucleus. The cell nucleus is protected by the membrane, which has nuclear pore complexes (NPCs) of diameter ranging from 20 to 160 nm. AuNPs conjugated with specific peptides having a nuclear localizing signal (NLS) can reach the cell nucleus. Several peptides have been identified as NLS peptides. Singh *et al.* showed that TAT conjugated PEG-AuNPs (10 nm) were internalized by MT4 lymphocytes (an HIV relevant cell line) and localized in and around the cell nuclei [46]. On the contrary, when larger size AuNPs (60 nm) conjugated with TAT peptides were used; NPs did not enter in cell nucleus [47,48]. It was found that an energy-dependent endocytosis process (clathrin and caveolae-mediated) was a key player in the cellular uptake of NPs [47,48] however, the NPs could not actively target the cell nucleus [48]. Brust's group investigated the role of multipeptides in delivering AuNPs to the cell nucleus. NLS, TAT and penetratin peptides appended to CALNN and conjugated on AuNPs were mostly found in the nucleus, cytosols and endosomes of HeLa cells [42]. Additionally, a large amount of NPs associated with the damaged endosomes was accumulated in the vicinity of the nucleus [42]. Further to improve the nuclear targeting, the multifunctional AuNPs conjugated with three peptides, including RGD to enhance the uptake, NLS to facilitate nuclear delivery and pentapeptide to protect NPs from

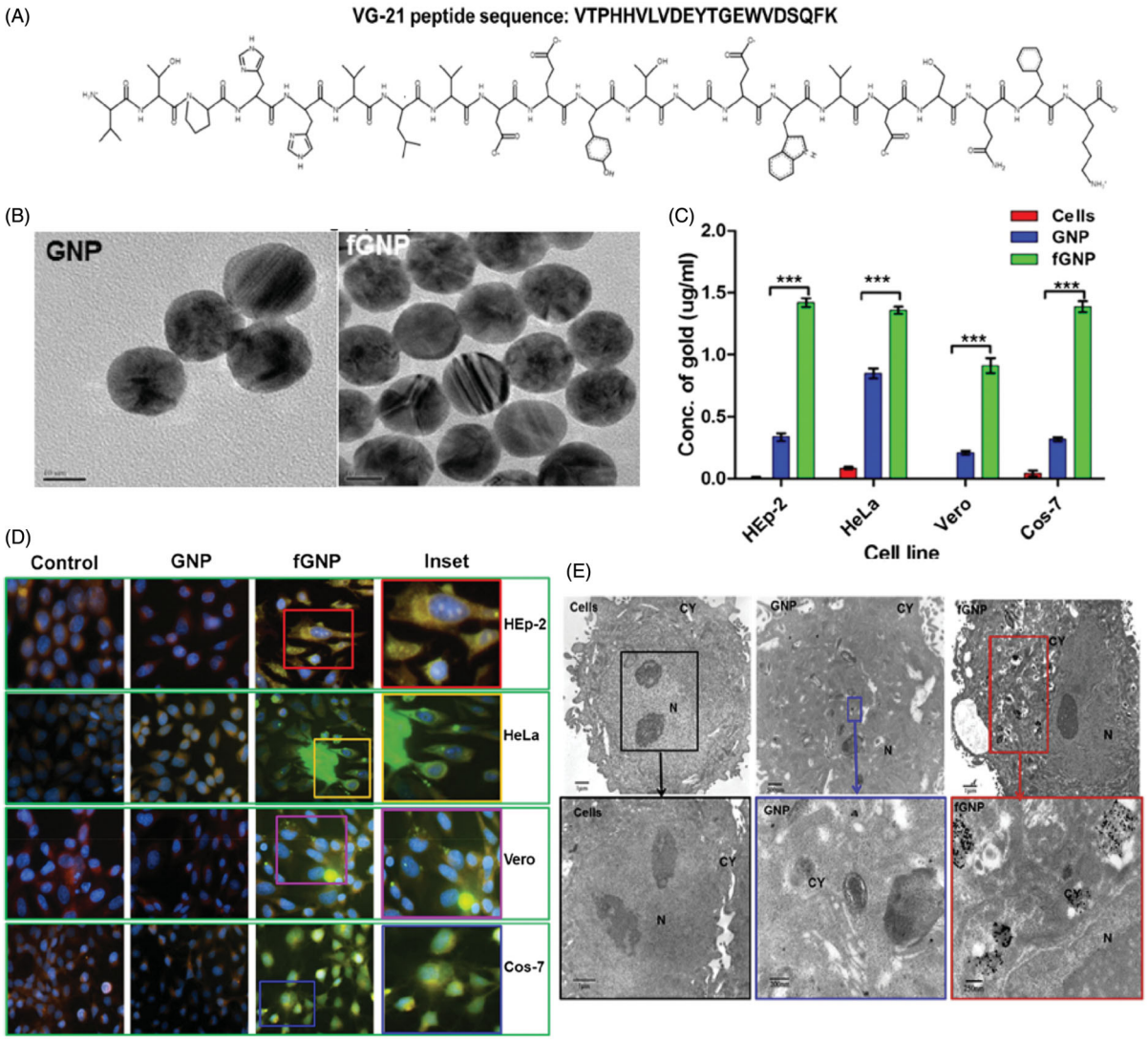

Figure 2. (A) Sequence and primary structure of VG-21 peptide. (B) TEM images of AuNPs and VG-21 peptide conjugated AuNPs. (C) Quantification of AuNPs and VG-21 peptide conjugated AuNPs internalized by cells. (D) Uptake of NPs was evaluated by Fluorescence microscopy. (E) TEM images of NPs internalized by HEp-2 cells. Adopted from Tiwari et al. [44].

protein corona effects, was developed to study the uptake and exocytosis of NPs, an important factor to exert their desirable applications (Figure 3) [49]. Peptide-AuNP conjugates showed a 5 fold cellular uptake followed by their localization in the cell's nucleus. The percentage of NPs exocytosed was lower by 2 fold for cells targeted with peptide-AuNP conjugates as compared to citrate-AuNPs. It was hypothesized that AuNPs capped with RGD and NLS peptides could reach the cytoplasm and nuclei of cells with a lower tendency to excrete it from there [49].

Delivery to subcellular location and endosomal escape

It is important to develop strategies to deliver cargos to subcellular organelles in order to achieve the promising outcomes. Ye *et al.* have explored the advantages of synergetic action of TAT and the membrane disruptive influenza virus hemagglutinin-2 (HA-2) peptides to improve cellular internalization, endolysosomal escape and the nuclear entry of NRs [50]. When TAT and HA2 conjugated with CALNN peptide either separately or both immobilized on self-assembled CALNN monolayer coated AuNPs (5 nm), the uptake of NPs significantly increased in HeLa cells. However, NPs could not escape the endolysosome. Increasing the molar ratio of the HA2 peptide or varying the direction of attachment of HA2 peptide onto the surface of NPs, resulted in an increased number of NPs inside the endosome but did not improve the release in the cell cytosol. This event happened due to overcrowding of the HA2 peptide on the surface of NPs that inhibited the conformational

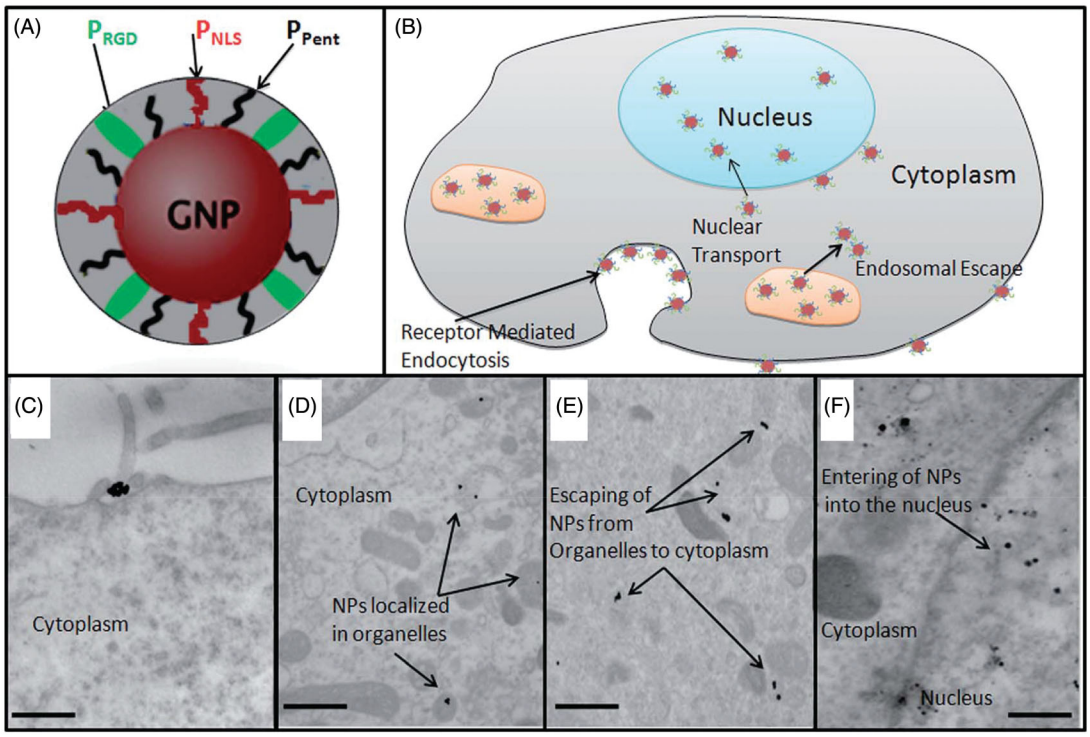

Figure 3. (A) Schematic of peptide functionalized AuNPs. (B) Trajectory of peptide functionalized AuNPs through cell. TEM images of peptide functionalized AuNPs bound to the plasma membrane for entry into the cell *via* the endocytosis process (C), internalized NPs localized in vesicles (D) escaping of NPs from vesicles into the cytosol (E) and entering of NPs inside the nucleus through the NPC (scale bars = 100 nm) (F) entering the nucleus through the NPS (scale bar = 100 nm). Adopted from Yang et al. [49].

changes of HA2 peptides necessarily for the endosome membrane destabilization [51]. On the other hand, the stearylated IFN7 peptide identified from N-terminus of HA2 facilitates endosomal escape of 160 nm AuNPs [52]. Interestingly, Wang *et al.* identified that the KDEL sequence, a highly conserved motif in the directed retrograde transport of proteins in the endoplasmic reticulum (ER), could be useful in the delivery of NPs by evading intracellular degradation [53]. CKDEL-AuNPs rapidly localized in the ER of Sol8 myogenic cells within 5 to 15 min. The majority of CKDEL-AuNPs were localized to ER after 1 h, which indicated that NPs were internalized *via* a clathrin-mediated pathway and trafficked to the ER *via* a retrograde transport pathway, avoiding the lysosomal degradation pathway.

Role of peptide density and diameter of NPs in cellular internalization

The density of peptides on the surface of AuNPs provides several tunable properties that can modulate the distribution of NPs inside cells. Medintz's group covalently conjugated CPP on a series of AuNPs ranging from 2.4 to 89 nm and found that NP uptake was directly dependent on the surface display of CPP. The ultimate cellular destination was determined by a diameter of NPs and the peptide density [54]. The smallest 2.4 nm NPs were found to be localized in the cell nucleus. Intermediate 5.5 and 8.2 nm NPs were partially delivered in the cytoplasm, however a portion of NPs appeared to remain at the cell membrane. 16 nm and larger NPs did not cross the cell membrane and mostly found at the cellular periphery [54]. However, when Sun *et al.* have functionalized the AuNPs (sizes 13, 30 and 60 nm) with CPP containing the CALNN derivative peptide ($CALNNR_8$); 13 and 30 nm NPs have higher cellular internalization than larger NPs (60 nm) by HeLa cells. The trend of intracellular distribution of NPs changes from nucleus to ER by increasing the density of $CALNNR_8$ on the constant diameter NPs [55]. Using both computational and experimental studies, it was shown that the concentration of AuNPs localized in the cell cytosol progressively increased with increasing the concentration of CALNN-TAT and CLPFFD-PPPPHKYLRW (PepN-Tf2) peptides on the surface of NPs up to 5.4 and 10% respectively, after that, the cytosolic concentration of peptide-AuNP conjugates started to decrease [56,57]. The high density of peptide conjugated on the surface of AuNPs reduces their ability to permeate the cell membrane by: (i) rendering NP unstable due to charge neutralization and (ii) causing

reduced mobility of peptides to adopt a favorable confirmation to interact with the cell membrane [56,57].

Effect of protein corona in cellular internalization

The role of media or serum is important in an internalization pattern of peptide-AuNP conjugates or the bare NPs because serum proteins could form the protein corona around the surface of NPs and therefore prevent the conjugated peptide to be recognized by the cell receptors. Wang *et al*. showed that the cellular internalization of CKDEL-AuNPs was reduced by SoI8 myogenic cells in the presence of serum as compared to the non-serum condition. Authors have not reported the stability of CKDEL-AuNP conjugates in the presence or the absence of serum-containing media [58]. However, in another study it was found that serum proteins helped the stability of peptide-AuNP conjugates in media containing several molecules and salts while media without serum promoted the aggregation of peptide-AuNP conjugates. It is worth noting that the cellular internalization pathway of aggregated AuNPs differs from the stable NPs which also controls the amount of internalized NPs [59]. Besides, Puntes's group investigated the role of surface charge NPs and serum protein in cellular internalization. For this purpose, they functionalized AuNPs with two peptides CIPGNVG-PEG-NH2 and CIPGNVG-PEG-COOH separately to provide the net charge at neutral pH. Human fibroblast cells (1BR3G) internalized more cationic AuNPs relative to anionic AuNPs, although no cytotoxicity was induced by both NPs. The predominant route of cellular internalization is endocytosis as confirmed by TEM analysis and the cationic NPs maintain the positive charge and the surface property in cell culture media in the first hour of the experiment. TEM images also confirmed the nuclear localization of some of cationic AuNPs [60].

Tumor and cancer therapy

The targeted delivery of drug conjugated NPs to solid tumors is a challenging task in nanomedicine for therapeutic and imaging applicatons [34]. The delivery of NPs to tumors is based on active and passive mechanisms however, there is still debate about the relative contribution of both mechanisms. No AuNPs-based drugs have been approved for clinical therapy. However, Auroshell NPs (Nanospectra Bioscience Inc) for NIR thermal treatment of head and neck cancers as well as TNF-α bound AuNPs (Aurimmune) and the combined taxol and TNF-α bound AuNPs (Auritol) were clinically tested for the treatment of solid tumors [61].

To enhance the killing efficiency of peptide-AuNP conjugates, pro-apoptotic peptide (PAP; $(KLALALK)_2$) conjugated AuNPs have been used to facilitate the killing of cancer cells by disrupting the mitochondrial membrane, resulting in cytochrome release and the induction of apoptosis [62,63]. In another study, a derivative of KLA peptide (WKRAKLAK), identified through prediction software and modified with α-lipoic acid (LA), was attached on AuNPs and AuNRs [64]. Anticancer activity of these formulations strongly depends on the size and shape of NPs, they being smaller NPs (20 nm) with higher uptake and stronger activity than that of larger NPs (40 nm) and AuNRs. The difference in activity could be attributed to the diameter of NPs and the peptide density on NPs/NRs, which influences the peptide configuration and ultimately the anticancer property of NPs/NRs [64]. Interestingly, tumor homing peptides (THPs) were identified through the phage display library and conjugated on AuNPs. THP-AuNPs target breast cancer cells (MCF-7), highlighting that peptides selected from the phage display technique can be used for tumor targeting irrespective of specific knowledge of target cell biology [65].

Radiotherapy and imaging

Radiotherapy is classified into internal radioisotope therapy using radioactive nuclides and external radiotherapy with remotely applied X-rays. Multifunctional NPs are considered to deliver several molecules at the same time for therapeutic and imaging purposes. Jimenez-Mancilla *et al*. have developed multifunctional AuNPs conjugated with CGC-Tat-BN, 1,4,7,10-tetraazacyclododecane-N,N′,N″,N‴-tetraacetic (DOTA)-GGC and hydrazinonicotinyl-FCDWKTCT (HYNIC-TOC) peptides through Au-thiol interactions [66]. ^{99m}Tc and ^{177}Lu labeling were performed *via* on the HYNIC-TOC ligand and DOTA-GGC respectively. The ^{177}Lu/^{99m}Tc-AuNP-Tat-BN systems selectively target tumor expressing gastrin-releasing peptide (GRP) receptors and kill them due to emissions of Auger and IC electrons vicinity to the DNA [66]. Similarly, cyclic RGD (cRGD)-^{177}Lu-Au NPs [67] and TC99m labeled AuNPs conjugated with FC131 peptide (target chemokine receptor-4 overexpressed in glioma cells) [68] were prepared to specifically target tumors in the animal models. These nanoformulations delivered the highest tumor radiation adsorb dose, leading to less tumor progression, less tumor metabolic activity, fewer intratumoral vessels and less VEGF gene expression than the other radiopharmaceuticals in mice due to their high tumor retention and the combined molecular targeting therapy and radiotherapy [67,68]. Rather than using radionuclides, Reshetnyak's group

had explored a very localized Auger effect of ultra-small AuNPs (1.4 nm), which can kill cancer cells upon X-rays irradiation [69]. pH-sensitive low insertion peptide (pHLIP) conjugated Au NPs (pHLIP-AuNPs, 1.4 nm) sensed acidity at the surface of the tumor and delivered NPs at the site of tumors. pHLIP-AuNPs tethered to the plasma membrane of tumor cells and triggered cell death by inducing oxidation of lipids, cholesterol and membrane proteins after radiation exposure [69]. Importantly, pHLIP-AuNPs selectively accumulated in tumors when administrated *via* either intratumoral or i.v. routes [70]. When pH insensitive k-pHLIP conjugated AuNPs was used, a significant reduction of AuNPs accumulation was found in the tumor, suggesting an important role of the acidic microenvironment of the tumor in pHLIP mediated targeting of ultra-small AuNPs [70].

Recently, cyclic-NGR (cNGR) and cRGD conjugated AuNRs were used as contrast agents to image tumors in U87 (positive $\alpha_v\beta_3$ integrin tumor), HT29 (negative $\alpha_v\beta_3$ integrin tumor) and subcutaneous 4T1 xenograft tumor models using X-ray CT and micro-CT technologies [71,72]. NGR and RGD-AuNRs rapidly and specifically bind to tumor vasculature after i.v. injection [72]. Notably, elastin peptide-AuNPs self-assembled in the chain like nanostructures inside the tumor of mice due to the increase in the local temperature in tumors upon the exposure of the NIR laser, enabling them to be used as a multimodal-imaging agent for photothermal/PA/X-ray-CT techniques [73]. In other multifunctional approaches, cRGD-polydopamine@AuNRs loaded with chelator-free iodine-125 (I^{125}) [74] and RGD-5poly(amidoamines) dendrimer@AuNPs loaded with gadolinium (Gd) chelator/(Gd (III) [75] were used as dual-mode nanoprobes for high-resolution-PA and CT/MR imaging in tumor-bearing mice models. High-resolution-PA imaging confirms that cRGD-polydopamine@AuNRs loaded with chelator-free iodine-125 (I^{125}) specifically targets tumor angiogenic vessels, which can be used as a potent tumor-therapy agent [74]. P75 peptides (a specific affinity to EGFR) conjugated PEG@Au nanotriangles (Au NTs) were developed as dual-modes CT/PA imaging agents to selectively target EGFR expressing non-small cell lung cancer cells (NSCLS). P75-PEG@AuNTs were used to treat NSCLS as a PTT agent under the real-time guidance of CT/PA imaging [76] (Figure 4). Additionally, Gong *et al.* used the positron emission tomography (PET)/CT technique to evaluate the migration of dendritic cells (DCs) in the lymphatic system of tumor-bearing mice using I^{124} labeled oligotyrosine (poly-Y-Rle)-Au NPs [77].

Receptor-mediated internalization

The main concern with the usage of NPs for cancer therapy is that only a small amount of NPs relative to the administration dose penetrates inside solid tumors. Therefore, the multiple administrations of NPs are required for satisfactory clinical outcomes. To specifically target cancer cells, receptor-mediated targeting of cancer cells has widely been explored using peptide-AuNP conjugates. Multifunctional AuNPs (2 nm) containing a therapeutic peptide (P12; TSFAEYWNLLSP) and a targeting peptide (CRGDK) for neuropilin-1 (Nrp-1) receptor has been developed for cancer treatment [78]. The P12 peptide is the most potent inhibitor that binds to MDM2 and MDMX complexes, which results in regulated activity and stability of the tumor-suppressing protein (p53), leading to limited expression of tumor genes and finally the cell apoptosis. CRGDK functionalization promotes the enhanced cellular internalization of AuNPs with P12 peptides due to the maximum binding interactions between CRGDK peptides and Nrp-1 receptors overexpressed on MDA-MB-321 cells [78]. Using a similar concept, the same group has developed CRGDK functionalized AuNPs loaded with Pt(IV) drug for prostate cancer treatment [79]. Targeted NPs are efficiently internalized in prostate cancer cells (PC3) using Nrp-1 receptor-mediated pathway, leading to accumulation of high dose of drugs and subsequent killing of cancer cells through the upregulation of nuclear factor kappa-B (NF-κB). In the interesting anticancer approach, Mustafa's group used AuNPs conjugated with modified RGD (RGDRGDRGDRGDPGC) and NLS (CGGGPKKKRKVGG) peptides to inhibit cancer cell migration due to enhanced nuclear stiffness [80]. It was found that AuNPs were trapped at the nuclear membrane and induced a high expression of lamin A/C protein, which is located in the inner nuclear membrane thus increased nuclear stiffness. In several other examples such as EphrinA2 (Eph2) [81], GRP [82–84] and urokinase plasminogen activator (uPAR) [85,86] receptors targeting peptide conjugated AuNPs have also been used for the targeted delivery of NPs in various cancer cell lines.

Albericio's group showed that the dual-peptide conjugated AuNPs containing both bombesin (BBN) and antitumor (RAF) peptides selectively inhibit the proliferation of HeLa cells overexpressing GPRs. BBN-RAF-AuNP conjugates do not recognize the non-GPR expressing neuroblastoma (SHSY-5Y) cells in vitro condition [87]. Moreover, tumor targeting in the animal model depends on the administration routes. Multipeptide AuNRs modified with three different ligands: (i) a single-chain variable fragment (ScFv) peptide that

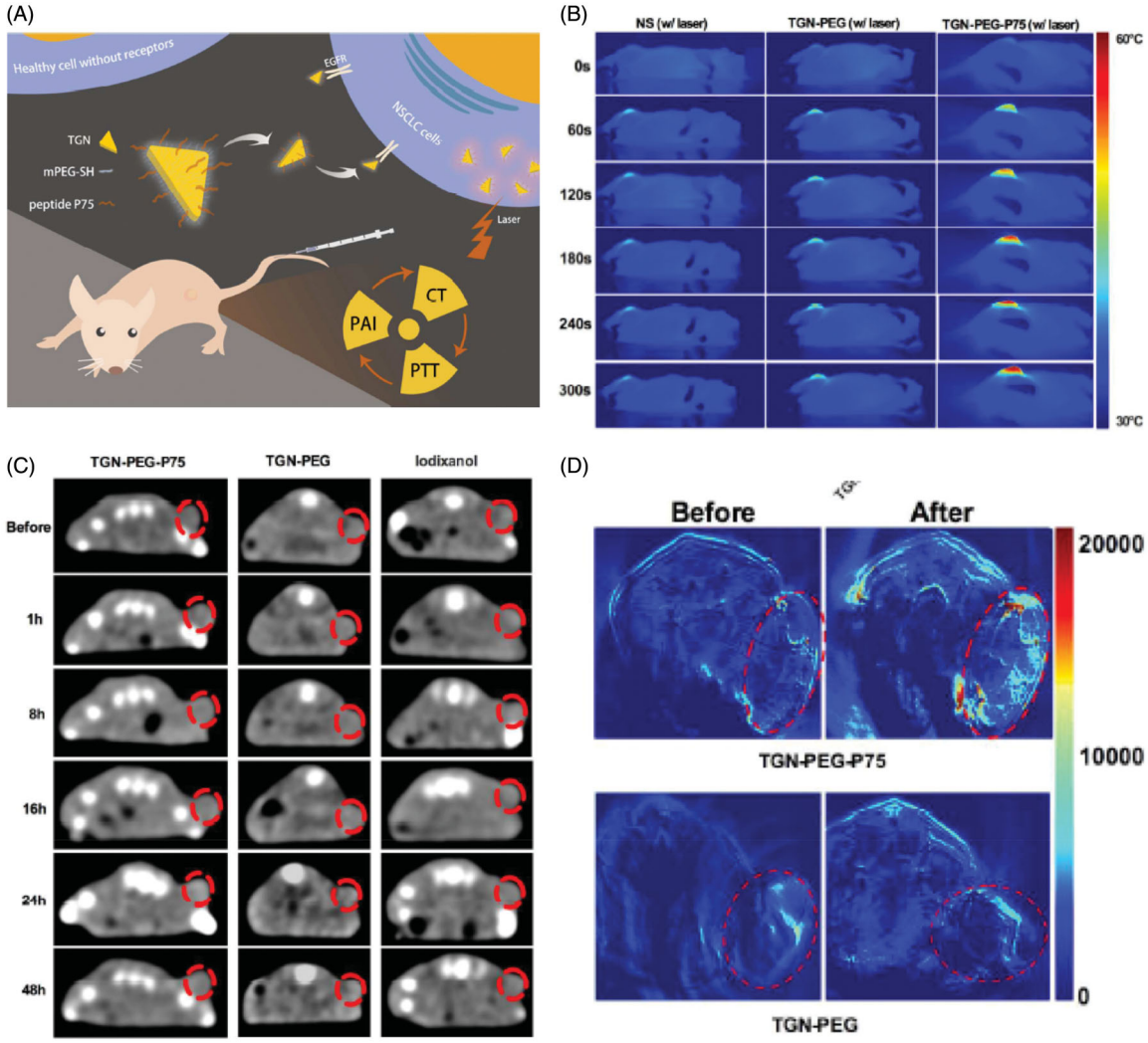

Figure 4. (A) Schematic representation of TGN-PRG-P75 and its applications for CT/PA imaging-guide PTT against NSCLC. (B) Photothermal images of HCC827 tumor-bearing mice exposure to irradiation (0.75 W/cm^2, 5 min) after intravenous injection with normal saline, TGN-PEG, and TGN-PEG-P75. (C) *In vivo* CT of tumor region before and at different time points post intravenous injection of TGN-PEG-P75, TGN-PEG, and Iodixanol (1 mg/ml, 200 μL, three mice per group). (D) Representative PA images of tumors on mice before and 24 h after intravenous injection with the TGN-PEG-P75 (1.0 mg/mL, 200 μL). The tumor areas were indicated by the red circles. Adopted from Zhao et al. [76].

recognizes the epidermal growth factor receptor (EGFR); (ii) an amino-terminal fragment (ATF) peptide that recognizes uPAR; and (iii) a cyclic RGD peptide, slightly improved the total Au accumulation in xenograft tumor models in comparison with non-targeted control [88]. When peptide conjugated NRs were delivered in mice *via* the i.v. route, the tumor microenvironments (*e.g.* fibroblasts, macrophages, and vasculatures) did not significantly influence the uptake of AuNRs by tumors. Additionally, it was found that peptide-AuNR conjugates were efficiently taken by RES organs (liver and spleen) after i.v. administration because they were less stealthy and recognized by the immune system for clearance. The delivery of NRs in tumors was limited by mass transport across the tumor vasculature at least for the rigid and large Au NRs. In the case of intratumoral administration, peptide-Au NR conjugates were found inside tumor or in tumor microenvironment, which depended on the nature of targeting ligands conjugated on these particles. Authors concluded that intratumoral instead of i.v. administration of peptide-AuNRs could be useful for cancer therapy [88].

Viral-mimicking peptide-AuNP conjugates

Taking advantage of viral infection mechanisms, several peptides have been derived from viral proteins to target cancer cells. 2 nm AuNPs conjugated with a 28-mer peptide corresponding to Hepatitis B virus-PreS1 protein (PreS1 (21-47)) can selectively target human hepatocellular carcinoma (HCC) and hepatoblastoma cells overexpressing SERPINB3 protein (SB3, also known as Squamous Cell Carcinoma Antigen 1, SCCA1) [89].

Similarly, a short therapeutic peptide (MDDRWPLEY TDDTYEIPW) derived from myxoma virus improved the targeting of 2.7 nm AuNPs to tumor cells in mice and also modulated the elimination of AuNPs by favoring renal over hepatic clearance (Table 1) [90].

Targeted drug delivery

To minimize offsite accumulation of cancer drugs and toxicity, the targeted delivery of drugs to cancer cells can be achieved using peptide-AuNP conjugates (Table 2). Mihara's group has developed a library of 16 peptides that have cell-penetrating property. Out of 16 peptides, 4 α-helical peptides have a nuclear targeting property similar to a TAT peptide. These α-helical peptides conjugated AuNPs (25 nm) were used to deliver anticancer drug doxorubicin (DOX; pH-sensitive DOX-PEG conjugate) to the nuclei of HeLa, A549 and 3T3-l1 cells, which induced cell death 2 times higher than the 41 nm size of the AuNP conjugated system [91,92]. Additionally, peptide-Au NP conjugates (41 nm) do not accumulate in the cell nucleus, which indicates that these NPs are not useful for the delivery of molecules inside the nucleus. To further improve the selectivity and the controlled release of DOX, a hybrid delivery system containing mesoporous silica NPs loaded with DOX and CALNNKKKRGD-AuNPs (4 nm) was developed, which exhibited pH-sensitive DOX release in endolysosomal vesicles of $\alpha_v\beta_3$ integrin overexpressing cancer cells [93]. Although CALNN peptides in combination with other biologically active peptides has been frequently used, their vulnerability to proteases limits the use of CALNN-AuNPs in the biological applications [94]. Keeping this issue in mind, Chauhan's group has synthesized a series of pentapeptides (derivative of CALNN) incorporating non-natural amino acid (α,β-dehydroxyphenylalanine, Δ Phe; and α -aminoisobutyric acid, Aib) [95]. Addition of Δ Phe and Aib in peptide sequences is well known to provide the increased resistance to peptides toward enzymatic degradation. The modified peptide conjugated AuNPs entrapped two anticancer drugs (DOX and Mitoxantrone) through hydrophobic interactions and delivered them to HeLa and L929 cells with the prominent toxicity. These peptides conjugated AuNPs are stable in the presence of proteinase K as compared to CALNN-AuNPs [95]. As an alternative approach, the P4 peptide isolated from the biopanning experiment was conjugated with chlorambucil (Chlor), melphalan (Melph) or bendamustine (Bend) drugs followed by loading on PEG-AuNPs. The peptide drug conjugate (PDC) loaded on PEG-AuNPs selectively targeted A20 murine lymphoma cells with the improved short half-lives as compared to the bare PDC [96]. Interestingly, Hou *et al.* have explored the delivery of DOX using phospho-peptide conjugated AuNPs [97]. Overexpression of phosphatases and abnormal tyrosine phosphorylation is characteristic of cancer cells. Phospho-peptide conjugated the AuNPs aggregate when phosphate groups are removed by phosphatases, leading to enhanced uptake by cancer cells [97].

Photothermal and photodynamic therapy

Hyperthermic therapy is a promising tool for the treatment of cancer using nanotechnology-based approaches. However, it is required that NPs should abundantly present near or inside cancer cells to achieve the substantial PTT effect. The exposure of photoresponsive AuNPs with the NIR laser of the specific wavelength facilitates the localized temperature increases and thereby photothermal killing of cancer cells due to the denaturation of biomolecules and cell damage. Tumor angiogenesis is the generation of blood vessels near the cancerous site to provide nutrient and oxygen that facilitates cancer growth. It is postulated that blocking the proliferation of blood vessels inhibits cancer growth, which could be complementary to current therapies. Anti-angiogenic P3 peptide (KATWLPPR) conjugated AuNRs that selectively bind to Nrp-1 receptor overexpressing human endothelial cells [98] and prevents tumor angiogenesis upon NIR laser exposure in a synergetic manner [99]. To specifically kill cancer cells, the YSA peptide conjugated Au nanoshell and AuNRs were used to improve their uptake by PC-3 cells and consequently enhanced the photothermal destruction of PC3 cells upon NIR laser exposure [81,100]. *In vivo* studies showed that photothermal destruction of breast tumors [101], non-small cell lung cancer (NSCLC) (Figure 4) [76], xenograft HeLa tumors [102] and subcutaneous tumors [73] were achieved using BBN-AuNRs, P75 peptide-AuNTs, spider venom peptide (lycosin-I)-AuNRs and elastin peptide-AuNPs respectively. Impressively, photoirradiation at the tumor site with 830 nm laser light at a power density of 2.5 W/cm^2 for 6 min led to the destruction of tumors without recurrence over 2 months [101]. It is believed that the NIR laser exposure in a small target volume (1 μm^3) generates nanobubbles (PNBs), resulting in the destruction of peptide-NP conjugates internalized cancer cells (Figure 5) [103].

Under the umbrella of the combined chemo-photothermal therapy approach, RGD-I^{125}-cisplatin loaded on polydopamine-AuNRs [74] and DOX loaded on RGD-Au nanostar-hollow mesoporous SiNPs [104] selectively accumulates in integrin expressing tumor cells and

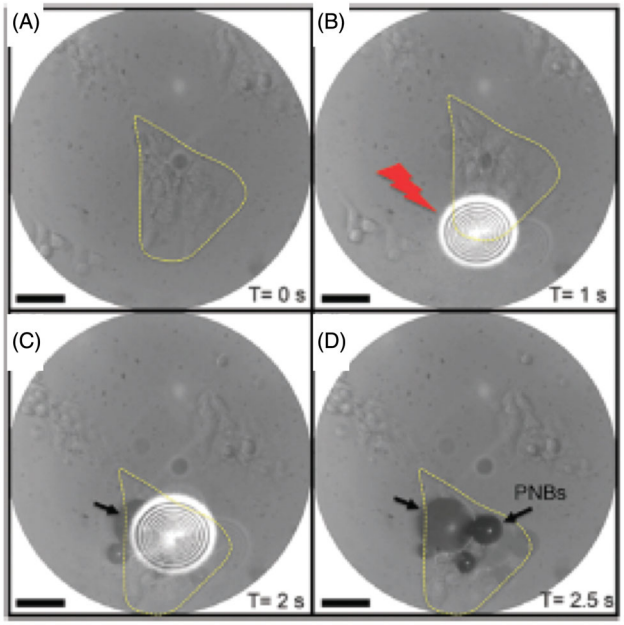

Figure 5. Generation of plasmonic nanobubbles (PNBs) in AuNR treated cells. (A) Bright field imaging of cells allowed us to select specific areas of cells to be irradiated (the selected area is highlighted by a yellow discontinuous line). Selected cells were irradiated with a laser with a beam spot diameter of 30 μm and at a fluence of 11.3 mJ cm^2 (B). After 2 s of irradiation (C) PNBs started to form. At 2.5 s irradiation was stopped and several PNBs were visualized within irradiated areas (D). Scale bars correspond to 100 μm. Adopted from Patino et al. [103].

targets tumor angiogenesis followed by tumor ablation in mice upon exposure of the NIR laser. Authors proposed that RGD conjugated AuNRs induced the change in cell morphology i.e. cytoskeleton protrusions such as lamellipodia and filopodia and therefore decreased the migration of cancer cells after the NIR laser exposure [105]. Additionally, photosensitizers such as: aluminum phthalocyanine (AlPcS4), protoporphyrin (PpIX) and phthalocyanine 4 (Pc-4) loaded on TAT/HA2 conjugated AuNRs@pNIPAAm, activatable cell-penetrating peptide (ACPP) conjugated AuNRs and EGF-AuNPs respectively had been used to kill the tumor in mice upon the exposure of light in a PDT approach [50,106,107]. ACPP has a matrix metalloproteinase-2 (MMP-2) sensitive peptide sequence (GPLGLAG), which is hydrolyzed by MMP-2 overexpressing tumor cells, leading to the release of the PpIX attached to CPP [106]. On the other hand, EGF-AuNPs enriched the tumor site due to the enhanced permeability and retention (EPR) effect, facilitating the delivery of a large quantity of Pc4 [108]. To improve the photothermal killing, chlorine6(Ce6)-pHLIP conjugated AuNRs (Ce6pHLIP-AuNRs) were developed as bimodal PDT and PTT agents [109]. Inside tumor cells, Ce6 molecules separate from AuNRs as a result of disulfide bond cleavage caused by intracellular glutathione (GSH) and produced singlet-oxygen species (for PDT) after the NIR laser exposure, causing the significant photothermal ablation of tumor cells [109]. As an alternative and eco-friendly approach, visible light has also been explored to arrest angiogenesis and kill PC3 cells using anti-angiogenic P3 peptide and PC3 cell-binding peptide (IAGLATPGWSHWLAL) conjugated AuNPs respectively, opening a new possibility to treat cancer cells [110,111]. For instance, the CAM model shows that visible light exposure leads to the generation of the localized high temperature, which destroys the blood vessels [111,112].

Research work discussed above seems to be promising for the treatment of cancer, but it is concerned that the outcomes of *in vitro* experiments do not translate in the animal models. Ghandehari's group showed that c-RGDfK conjugated AuNRs were internalized by DU145 prostate cancer cells and HUVECs *in vitro* condition. However, the tumor-targeting was not observed in tumor-bearing mice due to the fast clearance of NRs from the blood [113]. Similarly, ^{67}Ga labeled BBN conjugated AuNPs displayed excellent internalization (25% after 15 min) in the GRP receptor-expressing human pancreatic cancer cells. Biodistribution studies after i.v. and intraperitoneal (i.p.) injections of NPs showed that most NPs did not accumulate in the tumor of mice [114]. In another case, it was found that a larger size RGD-AuNPs-GD99mTC (80 nm) displayed the greatest effects *in vitro* model while on the contrary, a small size RGD-AuNPs-GD99mTC (29 nm) was a most effective to the *in vivo* model [115].

Targeting the blood brain barrier (BBB) and the treatment of brain/neurodegenerative diseases

With increasing life expectancy, brain-related diseases have become a major health problem globally. Diagnosis and treatment of brain diseases due to the limited crossing of drugs across the BBB requires the next-generation technology and the advanced drug delivery systems. BBB plays an important role in brain health and is often compromised in various diseases. BBB is considered as the main cause for the scarcity of therapies in the most neurological disorders due to their ability to restrict the delivery of many promising CNS drugs. To develop an effective cargo, Giralt's group showed that 12 nm AuNPs conjugated with or without radiolabelled ^{18}F-CLPFFD peptides that traveled to the rat brain after i.v. and i.p. injections. However higher amounts of CLPFFD-AuNPs were accumulated in the brain as compared to the bare NPs [116,117]. To

improve the accumulation of AuNPs, the same group has designed Tf (THRPPMWSPVWP)-CLPFFD peptide (Figure 6(A,B)) and the derivative of bicyclic peptide apamin (MiniAp-4, found in bee venom) and conjugated them to AuNPs (Table 1) [118,119]. Tf peptide targets the Tf receptor (TfR) expressed on the endothelial cells of the BBB and therefore promotes greater transcytosis of Tf conjugated AuNPs (10 nm) relative to PEG-AuNPs (10 nm) in both *in vitro* BBB and *in vivo* models (Figure 6) [118,120,121]. Tf peptide promotes the higher accumulation of Tf-conjugated AuNPs/NRs in the brain as compared to CLPFFD-AuNPs or PEG-AuNPs/NRs after i.v. administration (Figure 6) [118,120,121]. Importantly, we have reported that the exposure of NIR laser improves the transcytosis of Tf-AuNRs *in vitro* BBB and *in vivo* models as compared to other formulations due to the transient opening of BBB under the localized thermal effects (Figure 6(C–F)) [121]. The higher accumulation of peptide-AuNPs conjugates could be due to: (i) conformation and charges, (ii) hydrophobicity and (iii) the density of the conjugated peptide. Hydrophobicity and the density of conjugated peptides allow better interactions with cell membrane and receptors [118,121]. On contrary, it was also shown that CLPFFD-AuNPs (1.4 nm) impeded transcytosis across the BBB, indicating that the choice of a specific size of AuNPs is an important key for biomedical applications [122].

The most commonly used RGD peptide was also explored to target brain cancer cells. RGD-AuNPs traveled to the brain of the intracranial tumor and orthotopic brain glioma models, and the amount of RGD-AuNPs was significantly higher than that of untargeted bare AuNPs [123,124]. Moreover, RGD-AuNPs loaded with Mn chelates were also used as a dual-modal MR/CT imaging agent for orthotopic brain glioma [124]. In a multifunctional approach, glucose coated AuNPs (2 nm) carrying two neuropeptides (either pentapeptide YGGFL (Enk) or the glycosylated peptide (GGGYTGFLS-O-β-glucoside (Glycopep)) and a chelator of positron emitter ^{68}Ga as a PET reporter, were developed to enhance the BBB transcytosis and to track the bio-distribution of NPs in the brain [125]. The targeted ^{68}Ga-AuNPs with Enk peptide improved BBB permeation and brain accumulation nearly 3 fold (0.02%ID/g) when compared to the non-targeted AuNPs (0.0073% ID/g), as measured by the PET technique [125].

Delivery of hydrophobic drugs is a huge challenge for the treatment of brain cancer because only a small percentage of administered drugs reach to brain. EGF-AuNPs [126] and Tf-AuNPs [127] facilitate 10 and 6 fold improved accumulation of hydrophobic Pc4 drugs respectively in brain tumor-bearing animal models. The untargeted Au NP conjugates have a little offsite accumulation in other organs. *In vitro* study showed that Pc4-Tf-AuNPs was significantly internalized by Tf overexpressing human glioma cancer lines (LN229 and U87 cells) and accumulated within mitochondria of tumor cells [127]. In a dual-mode therapy and imaging approach, TAT-AuNPs loaded either with DOX or the combination of DOX and Gd^{3+} contrast agent efficiently delivered a DOX and Gd^{3+} chelator to intracranial glioma xenografts-bearing mice, leading to a significant survival benefit and enhanced brain tumor imaging due to the prolonged retention time of Gd^{3+} [128,129].

To explore dual-mode PTT and imaging approach, hollow Au nanospheres (HAuNSs) functionalized with c(KRGDf)-PEG-SH (c(KRGDf)-PEG-SH-HAuNS) were used both in photothermal ablations of cancer cells by increasing tumor temperature by 20.7 °C and in highly sensitive PA molecular imaging [130]. It was found that PTT treatment significantly elevated the survival of tumor-bearing mice by killing the glioma cells. After 24 h of nanoformulation administration, the PA signal ratio of tumor to the contralateral normal brain was 2 times higher than that of the precontrast agent, demonstrating the selective accumulation of NPs in the tumor. microCT/PET techniques also validated the accumulation of NPs in the tumor [130].

The abnormal protein misfolding, along with the formation of insoluble fibers and amyloidogenesis have prominent roles in devastating neurodegenerative diseases such as Alzheimer and Parkinson. Puntes's group showed that amphipathic peptide CLPFFD conjugated AuNPs was able to eliminate the toxic β-aggregates involved in Alzheimer's diseases (AD) *in vitro* conditions [131]. CLPFFD peptide recognizes the hydrophobic domain of oligomers, protofibrils and fibrils, which are β-amyloid toxic protein aggregates (Aβ), and blocks the amyloid fiber growth at its higher concentration. Remotely applied low energy microwave fields (0.1 W) at different stages of growth of fibrils attached with CLPFFD-AuNPs led to adsorption of energy by NPs followed by the dissipation of heat, causing disaggregation of amyloid deposits and aggregates. The products formed after irradiation were not amyloidogenic and did not allow the formation of amyloid fibers after the addition of fresh Aβ precursors [131,132]. When the CLPFFD sequence was changed to CDLPFF and CLPDFF sequences, these two sequences exhibited poor affinity with Aβ fibrils, given that the position of negatively charged amino acids and their poor capacity to adopt suitable secondary structures on the surface of AuNPs

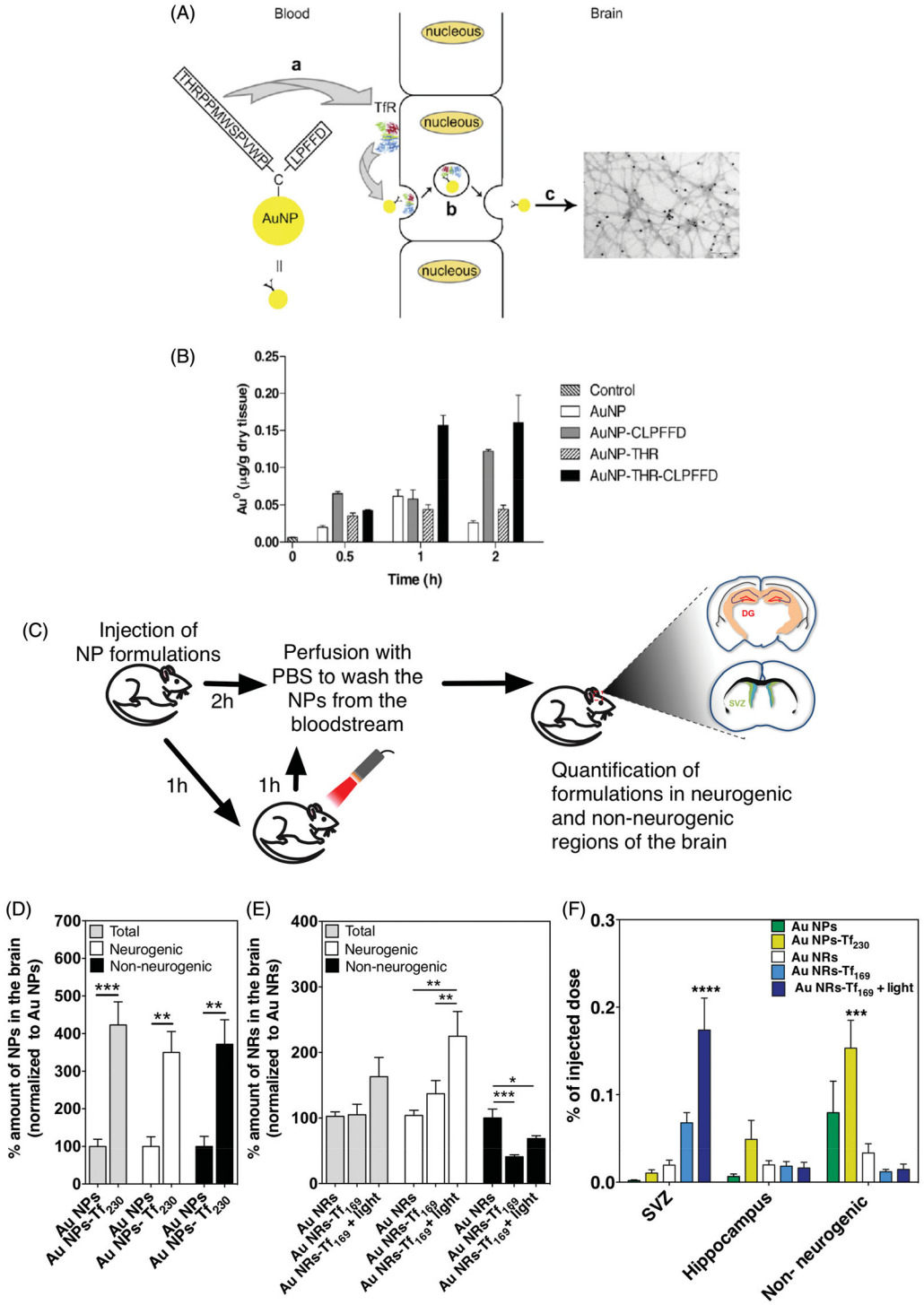

Figure 6. (A) Scheme to rationalize the design of the conjugate AuNP-THR-LPFFD: (a) THR-CLPFFD peptide anchored to the AuNP. This peptide contains the THR sequence that recognizes the transferrin receptor and LPFFD that recognize Aβ aggregates; (b) transport of the endocytic vesicle through the endothelial cells of the blood brain barrier; and (c) recognition and binding of the conjugate to Aβ aggregates inside the central nervous system. Transferrin receptor is abbreviated as TfR. (B) Gold content in rat brains after injection of nanoparticles. Animals were perfused gently with PBS before organ extraction. The gold content was determined by neutron activation. The experiment was repeated with four animals. (C) Scheme illustrating the methodology used. In case of Au NRs, the animals were exposed to a NIR laser (2 W/cm^2 for 2 min) at time 1 h. 2 h post-injection, the animals were sacrificed and the different brain regions were collected for ICP-MS analysis. (D and E) Quantification of formulations (Au NPs or Au NRs) in total brain, neurogenic (SVZ and hippocampus) and non-neurogenic (cortex) regions, using ICP-MS analyses. (F) Quantification of Au content for each condition in the different regions normalized to the initial Au administrated (1 mg per animal, which corresponds to 780 μg of Au NPs and 144 μg of Au NRs). Results are average ± SEM ($n = 6$-9 animals). $^{**}p < 0.01$, $^{***}p < 0.001$ and $^{****}p < 0.0001$. Adopted from Prades et al. [118] and Praca et al. [121].

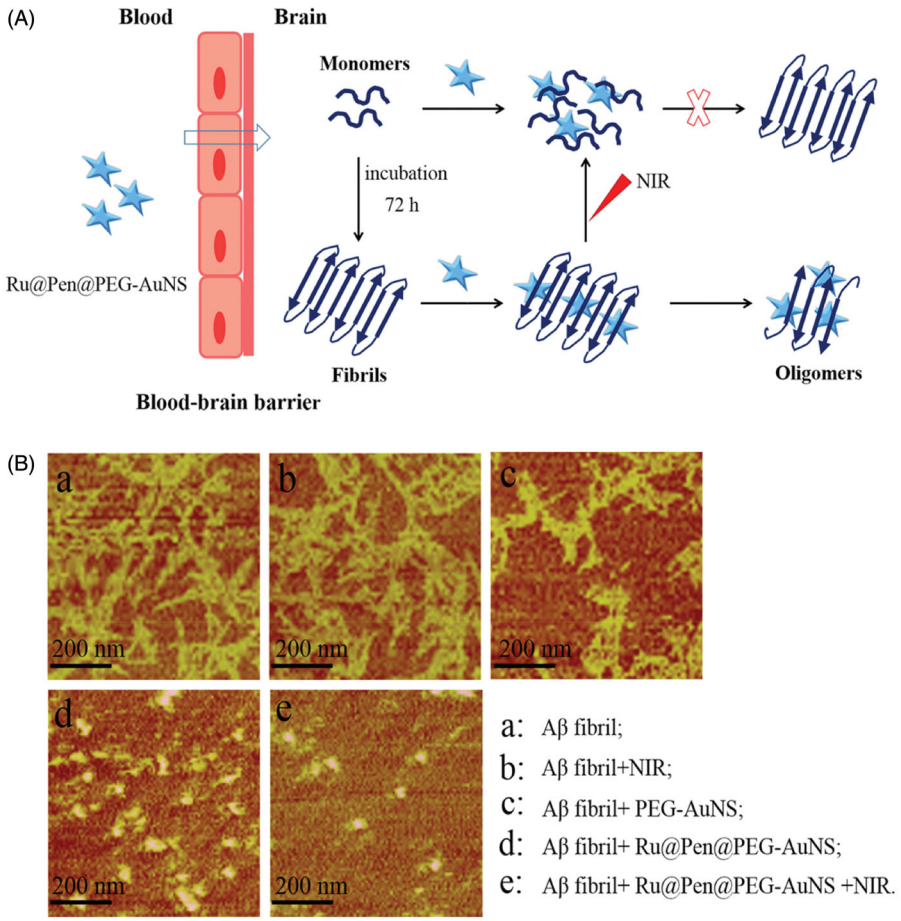

Figure 7. (A) Schematic representation of penetratin conjugated AuNSs to cross BBB and disassembly of Aβ aggregates under NIR laser exposure. (B) Structural changes of Aβ fibrils using AFM images of Aβ fibrils, alone or treated with PEG-AuNS and Ru@Pen@PEG-AuNS (20 μg/mL) in the absence or presence of 3 min NIR irradiation (0.75 W/cm^2, 808 nm). Adopted from Yin et al. [135].

[133]. Intriguingly, Xiong *et al.* proposed a simple approach to combine two peptide inhibitors VVIA and CLPFFD into one peptide sequence to strongly inhibit the formation of Aβ aggregates and to reduce the cytotoxicity caused by aggregates. The hybrid peptide VVIACLPFFD (VCD10) conjugated AuNPs exhibited the superior inhibition activity against $A\beta_{42}$ aggregates with increasing cell viability from 48 to 82% when compared to the individual peptide (VVIA or CLPFFD) conjugated NPs [134]. The superior activity of VCD10 conjugated AuNPs could be due to its dual-inhibitory sequence, special surface orientation and conformation [134]. In recent years, taking advantage of the tissue penetration window of NIR laser, the PTT approach was explored to disassemble the aggregated amyloid fiber and to inhibit the formation of fibrils in both *in vitro* [135–137] and *in vivo* [135,137] models using penetratin conjugated Au nanostars (AuNSs), CLPFFD conjugated HAuNSs and AuNRs and Aβ15-20 peptide conjugated AuNRs (Figure 7).

Modulation of immune response for the treatment of different diseases

Despite the rapid development of several strategies to conjugate various peptides on the surface of AuNPs, there is a little knowledge about their immunological responses. In this direction, Puntes's group reported that the immunological response of peptide (CLPFFD, CDLPFF, CLPDFF and $C(VRLPPP)_3$) conjugated AuNPs (10 nm) depended on the peptide sequence, hydrophobicity and their packing arrangement on the surface of AuNPs [20]. It was observed that macrophage proliferation and secretion of cytokines were independent of the particle size, charge and composition but not on the peptide coating order. These results suggested that it was possible to modulate the immune system to produce a different defense or immune response by modifying the sequence of peptides [19,20]. Furthermore, Turvey's group prepared a library of 6mer peptides, including CLPFFD and CLPAAD peptides. AuNPs (13 nm)

were conjugated with single or binary mixtures of peptides [138]. Among 10 NP hybrids, CLPFFD-AuNPs (P12-AuNPs) strongly inhibited both NF-κB-AP1 and IRF3 activation in macrophages while no inhibition was found for CLPAAD-AuNPs (P13-AuNPs). It was suggested that hydrophobicity and the aromatic ring structure of the amino acid present in the peptides were responsible for modulating TLR4 response [138,139]. Additionally, P12-AuNPs were effective in reducing inflammation to the *in vivo* model of intestinal inflammation while P13-AuNPs was biologically inactive (Figure 8) [140].

In the last few years, immunotherapy has been considered to be a potent weapon for cancer treatment. Peptides having sequences from the luteinizing releasing hormone (LHRH; B and T cell epitope) and T-helper epitopes were modified at N-terminus with palmitoyl and acetyl groups as well as C-terminus with Cys amino acid [141]. The peptide-AuNP conjugates targeted to FcRs of human DCs were effective as antigen delivery carriers and induced strong immune responses with respect to non-targeted LHRHTT-AuNPs, indicating their potentials as cancer vaccines [141]. Similarly, Poly-Y-Rle-AuNPs induced a strong antitumor immunity including the expression of CD8+ cytotoxic T lymphocytes (CTL) precursor and CTL mediated cytotoxicity against cervical cancer with IL-6 and TNF-α production in tumor-bearing mice model [77]. To look for another immunological target to open a new avenue for the cancer prophylaxis, Mocan *et al.* hypothesized that MUC-1 (CD227), a membrane tethered mucine glycoprotein, could generate an adequate immune response. MUC-1 peptide-AuNPs activate peritoneal macrophage cells, resulting in the release of TNF-α, IL-6, IL-10 and IL-12 cytokines. MUC-1 peptide-AuNPs polarize macrophages to M1 phenotype, which is important for antigen presentation and vaccine development [142]. Moreover, a chimeric peptide consisting of MUC-1 and T-cell epitope P30 sequence conjugated on AuNPs induced the significant MHC-II mediated immune response *in vivo* model and their antisera recognized human breast cancer cells *in vitro* condition [143]. Overall, peptide conjugated AuNPs can induce the major immune activation without the need of adjuvant in both *in vitro* and *in vivo* tumor models, highlighting their potential as vaccine candidates [144,145].

Taking cues from viral and bacterial proteins that act as antigens to induce the production of antibodies, several active peptides have been identified from these proteins, which could act in a similar fashion. Peptide-AuNP conjugates have been considered as immune modulators and vaccines to fight against viral and bacterial infections. Au NPs conjugated with peptides derived from Epstein-Barr virus (EBV) [146], foot and mouth disease [147,148] and HIV [149] induced a very strong immune response in both *in vitro* and *in vivo* models. It is found that an immune response depends on the size of AuNPs and the stability of the secondary structure of conjugated peptides [147,149]. In another interesting study, 60 and 80 nm AuNPs were conjugated with ovalbumin peptide (OVAp) and CpG oligonucleotide that stimulated TLR9 respectively [150]. It was shown that 60 nm OVAp-AuNPs promoted the greatest level of antigen presentation by DCs while 80 nm CpG-AuNPs led to the greater expression of activation markers. Further, mice were administered with NanoAu-cocktails treated DCs to induce immunization 5 days before the injection of liver infection inducing virus. Results showed a significant reduction of viral load in the liver as compared to the control mice, indicating the enhanced protection provided by the activated immune systems (Figure 9) [150]. Additionally, AuNPs carrying a synthetic tetrasaccharide epitope related to the *Streptococcus pneumoniae* type 14 capsular polysaccharide (Pn14PS) and T-helper ovalbumin 323-339 peptide (OVA(323-339)) [151], or flagellin peptide (highly conserved N-terminus domain of *Pseudomonas aeruginosas*) [152] elicited suitable antibodies in mice, leading to the prevention of bacterial infections.

Oligonucleotide (gene) delivery

Cationic AuNPs not only bind and condense oligonucleotides but also deliver them inside cells. Although, several molecules such as PEI, PAMAM dendrimers, and polyL-lysine conjugated to AuNPs have been used to deliver various types of oligonucleotides, their specificity and selectivity are poor to cells. Conversely, peptides having the advantages of targeting to specific cells are explored in combination with AuNPs to deliver, DNA, miRNA and siRNA (Table 2). Mirkin's group developed peptide antisense AuNPs by mixing the thiol terminated oligonucleotide and peptide terminated with N-terminal cysteine in different molar ratios in an AuNP solution to achieve different loadings of both molecules on the surface of NPs [153]. It was found that the addition of salts was necessary to screen the electrostatic interactions between peptide and oligonucleotide and to prevent aggregation of NPs. *In vitro* studies showed that nanoconjugates entered inside cells and controlled the gene regulation [153]. In another case, CKDEL-AuNP platform was developed to deliver NADPH oxidase isoform 4(Nox4) siRNA to both undifferentiated C2C12

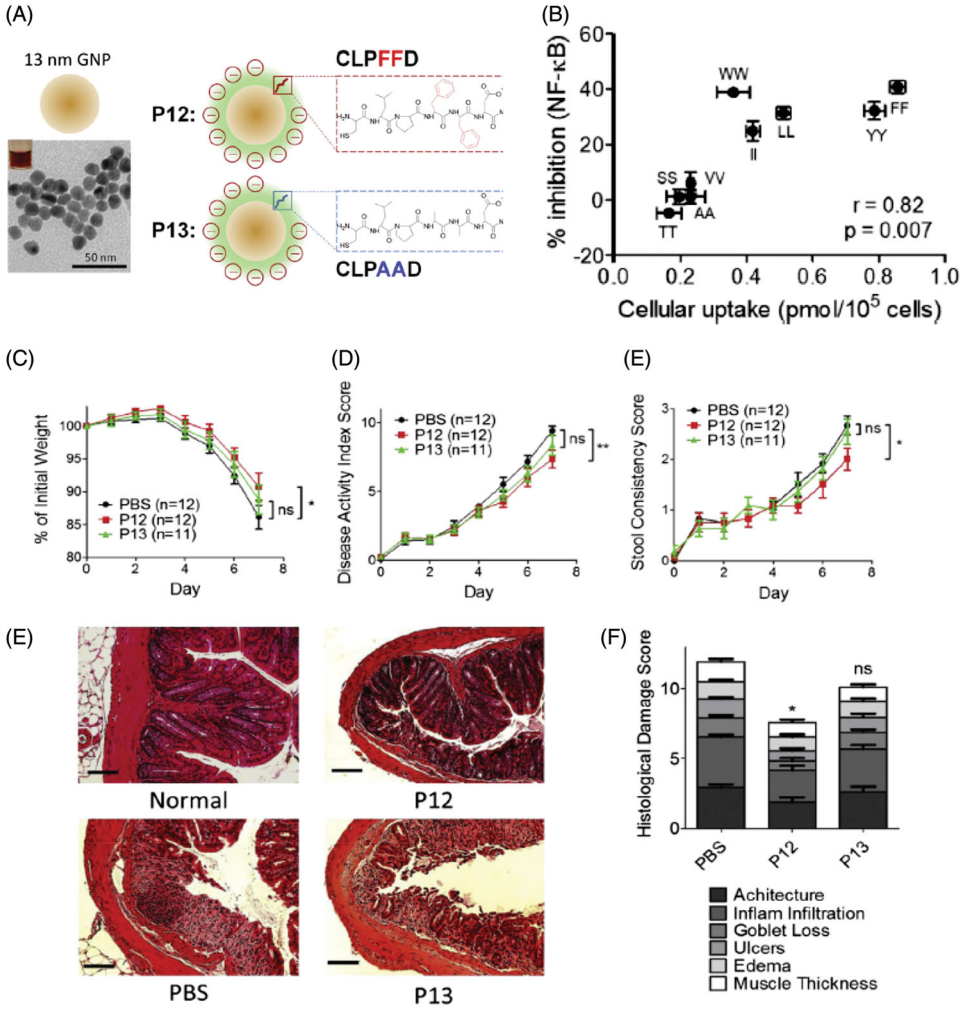

Figure 8. (A) A scheme showing the amino acid sequences of the peptides conjugated on the GNP surface. The middle XX region could be amino acids with hydrophilic side chains such as serine (SS) and threonine (TT), or hydrophobic side chains, such as alanine (AA, P13), valine (VV), leucine (LL), isoleucine (II), tyrosine (YY), tryptophan (WW), or phenylalanine (FF, P12). (B) Correlation of the cellular uptake of various peptide-GNP hybrids and their inhibitory activity on NF-kB Correlation coefficient (r) is equal to 0.82 ($p = 0.007$) for NF-kB inhibition. Evaluation of the therapeutic efficacy of nanoparticle P12 in the DSS-induced mouse model of intestinal inflammation. Nanoparticle P12 treatment improved the disease severity and dampened intestinal inflammation, as indicated by: reduced weight loss (C), disease activity indices (D), stool consistency (E), H&E stained colon sections (F) and histological damage scores (G). Scale bar = 100 mm; $^{*}p < 0.05$; $^{**}p < 0.01$; ns: not significant. Adopted from Yang et al. [140].

myoblasts and differentiated C2C12 myotubes [154]. The cellular uptake of NPs was more efficient than lipofectamine (LF) mediated transfection in differentiated myotubes. The most of siRNA was localized in the ER with minimal distribution in the Golgi bodies in undifferentiated myoblasts, suggesting that the ER was a primary localization site for KDEL-AuNP mediated delivery of siRNA [154]. For the treatment of atherosclerosis, vascular cell adhesion molecule (VCAM-1) binding peptide conjugated AuNPs was employed to deliver anti-athero-miRNAs (miR-712) specifically to inflamed endothelial cells (overexpressing VCAM-1 receptors) to inhibit the formation of atherosclerotic plaques [155].

Stem cell engineering

To modulate stem cell activity, AuNPs functionalized with a zwitterionic N-Cys-Ku70 pentapeptide (derived from a Bax inhibiting peptide) was loaded with a 6.6 Kbp gene designed to express BDNF/m-cherry fusion protein [156]. The genetically modified mesenchymal stem cells (MSCs) exposed to the NP construct exhibited protein expression of BDNF/m-cherry within 4 days without inducing any cytotoxicity, showing a new non-viral method for MSC engineering [156]. Mao's group reported that PEP (an antimicrobial peptide; AMP) conjugated on PEI capped AuNPs can be used to deliver luciferase reporter genes to MSCs (Figure 10) [157].

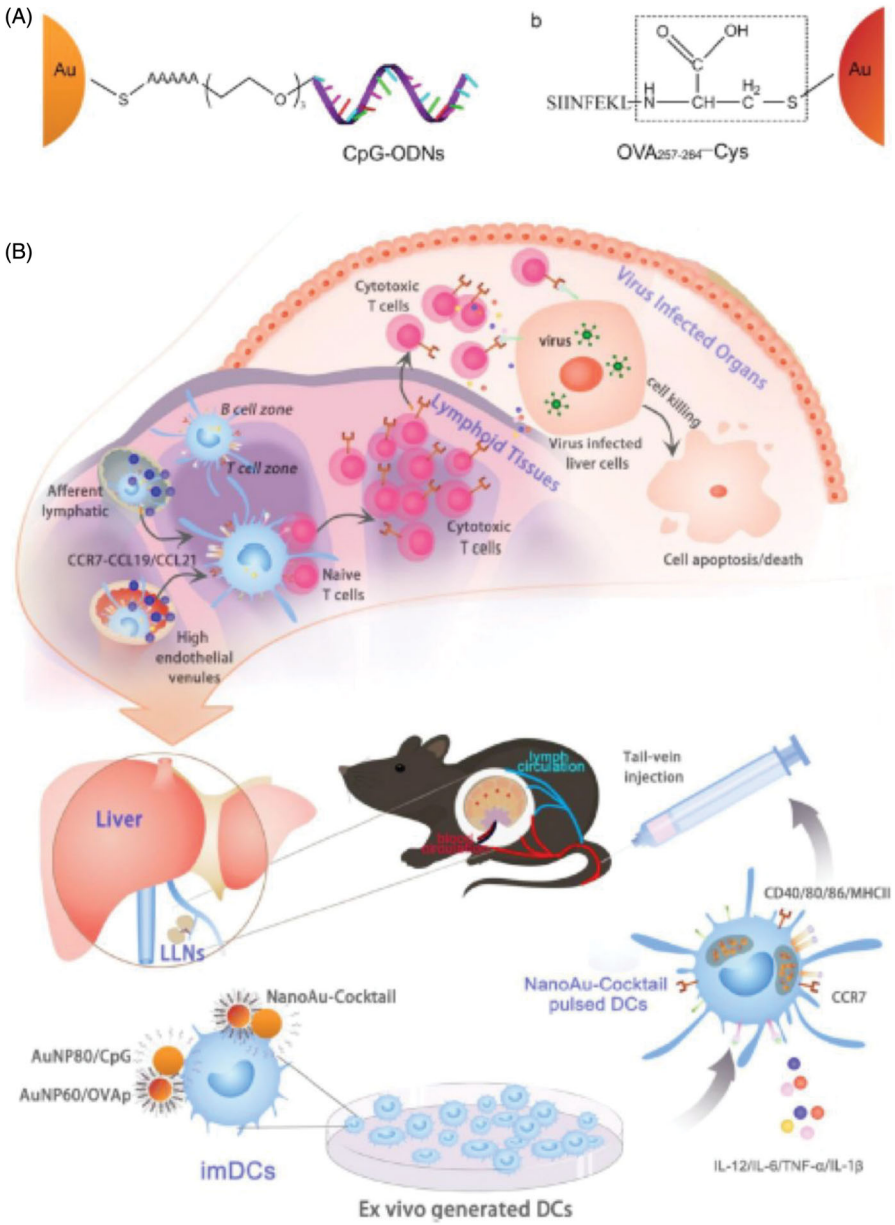

Figure 9. (A) Schematic diagram of chemical modification of AuNPs modified with CpG oligonucleotide and OVAp through the Au-S bond. (B) Schematics representing the mechanisms of NanoAu-cocktail pulsed DCs induction of antiviral T cell responses. Adopted from Zhou et al. [150].

Cationic AMP aids in cellular internalization of AuNPs and also promotes condensation of genes on the surface of AMP-AuNPs. High transfection efficiency in both *in vitro* (100 times higher than PEI-AuNPs) and *in vivo* (gene encoding VEGF) was observed in the presence of PEP-PEI-AuNPs (Figure 10) [157]. The same group also showed that the TAT-PEI-AuNPs had high efficiency in transfecting rat epidermal stem cells (ESCs) without inducing cytotoxicity as compared to PEI-Au or TAT-AuNPs. TAT-PEI-AuNPs loaded with plasmid DNA (pDNA, which encodes basic fibroblast growth factor (FBS)) differentiate ESCs into neuronal cells with the expression of several neuronal markers [158].

Cancer therapy

For the targeted cancer therapy, cRGD was employed as a targeting ligand for AuNPs mediated delivery of siRNA to silence the papilloma virus-derived E6 oncogene. To prepare the unimer polyion complex-AuNPs (uPIC-AuNPs), cRGD installed poly(ethylene glycol)-block-poly(l-lysine) modified with lipoic acid (cRGD-PEG-PLL-LA) was assembled with siRNA followed by the decoration on AuNPs. This system enhanced gene silencing *in vitro* and decreased the tumor size in subcutaneous HeLa tumor-bearing mice models [159,160]. Taking advantage of cell-penetrating and biocompatible profile of TAT peptide, Gong *et al.* and Niu *et al.*

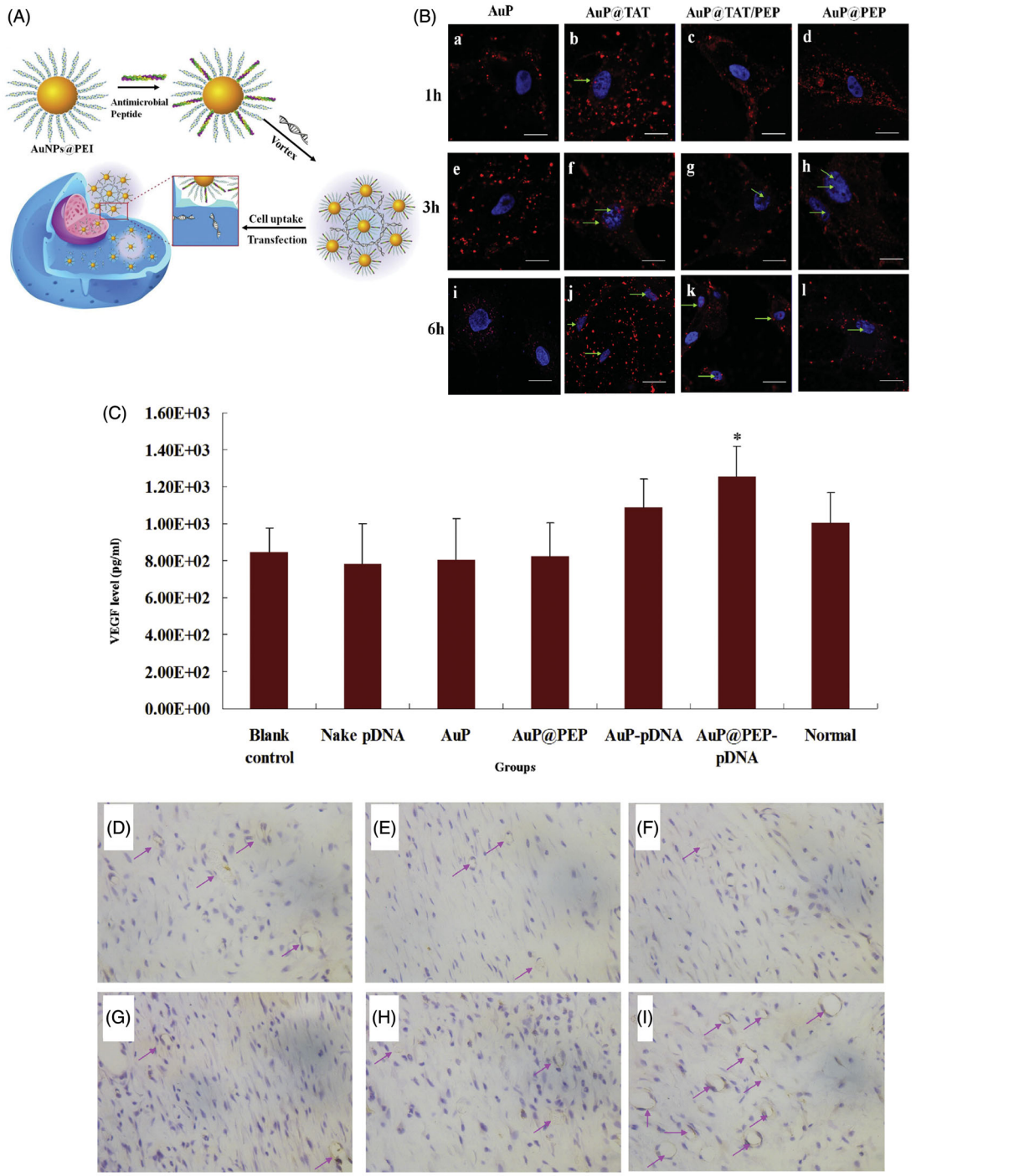

Figure 10. (A) Schematic illustration of the preparation of PEP and/or TAT peptide conjugated cationic AuNPs and their interaction with pDNAs and cells. (B) CLSM images of cells treated with (a, e, i) AuP/pDNA complexes, (b, f, j) AuP@TAT/pDNA complexes, (c, g, k) AuP@TAT/PEP/pDNA complexes, and (d, h, l) AuP@PEP/pDNA complexes for (a, e, d) 1 h, (e-h) 3 h and (i-l) 6 h, respectively. The peptide contents of AuP@TAT, AuP@TAT/PEP, and AuP@PEP are about 2.5%. Scale bar is 5 mm. Arrows indicated Cy3-pDNA inside cell nucleus. (C) The VEGF levels within homogenized tissues treated with different vector/pDNA complexes. *Indicates significant difference at $p < 0.05$ level, vs blank control. Optical micrographs of CD31-stained sections of the newly formed tissues in SD rats 14 days post-surgery, treated with (D) saline, (E) naked pDNA-VEGF, (F) AuP, (G) AuP@PEP, (H) AuP/pDNA-VEGF, and (I) AuP@PEP/pDNA-VEGF, respectively. The peptide contents of AuP@TAT, AuP@TAT/PEP, and AuP@PEP are about 2.5%. Scale bar is 50 mm. Arrows indicate vessel-like structures. Adopted from Peng et al. [157].

loaded antisense oligonucleotide (ASO) and pDNA-Mi221 on TAT-AuNPs respectively. These nanoconstructs induced significant reduction of metastasis tumor nodules and cutaneous melanoma in the animal model [161,162]. Therefore, TAT-AuNPs could be used as an efficient carrier for transdermal delivery of oligonucleotide, indicating a novel topical gene therapy strategy for the notorious skin cancer [162]. Recently, spatial-temporal controlled delivery of drugs in living cells to modify cellular functions is of great interest to treat cancer. Braun *et al.* demonstrated the NIR dependent release of siRNA from TAT-lipid coated Au nanoshells [163]. The coating of TAT-lipid facilitates cellular internalization of nanoshell in picomolar concentrations, avoiding undesired cytotoxicity of Au nanoshells. Notably, time and power-dependent NIR laser induced the release of siRNA through Au-S cleavage while the escape of siRNA from endosomes occurred above the critical pulse energy exposure, which was attributed to the local heating and the cavitation that led to the rupture of the endosomal membrane.

Antimicrobial peptide-AuNP conjugates

Antimicrobial peptides (AMPs) have been considered as alternatives to antibiotics as potential therapeutic drugs due to the development of antibiotic resistance bacteria [164,165]. Until now, more than 800 AMPs have been isolated from fungi, bacteria, insects, vertebrates and plants that can kill a broad range of microorganisms. Recently, hybrid CM peptide (Figure 11(A–D)) [166] and esculentin-1a(1-25)NH_2 [Esc(1-21), isolated from Frog skin] [167] were covalently conjugated on SPION-Au core-shell NPs (CM-SPION@AuNPs) and AuNPs respectively. CM-SPION@AuNPs have a potent antimicrobial activity to kill both Gram-positive and Gram-negative bacteria with a very low minimum inhibitory concentration (MIC) than the soluble peptide [166]. The CM-SPION@Au core-shell NPs was used multiple times to kill bacteria without losing the antimicrobial activity. These NPs were biocompatible to human cells, indicating that the conjugated CM peptide is selective to kill bacterial cells. It was found that CM-SPION@Au core-shell NPs caused protrusions and blisters in the bacterial membrane after 4 h of incubation. CM-SPION@Au core-shell NPs were located in the periplasmic space of *E. coli* [166]. Interestingly, Esc(1-21)-AuNPs rapidly clustered around the *P. aeruginosa* membrane after 1 min and led to membrane breakage after 8 min of incubation [167]. With further emphasis on infection control, His-tagged DNA aptamer-AuNPs (Apt-AuNPs) were conjugated with C-terminal hexaHis tagged A3-APO-AMP. These nanoconstructs killed *Salmonella* typhimurium (*S.* Typhimurium) in *S.* Typhimurium-infected HeLa cells, resulting in the increased viability of host cells. The i.v. administration of nanoconstructs in *S.* Typhimurium infected mice resulted in 100% survival of mice due to complete inhibition of *S.* Typhimurium colonization [168]. In this direction, Peng *et al.* showed that PEP, an AMP conjugated on PEI-AuNPs had superior antibacterial property as compared to the free peptide [157]. PEP has a sequence from lactoferrin, an iron-binding protein from the native innate immune system, with antifungal and antibacterial property [157]. For the effective treatment of infected wounds, surfactin (SFT), a cyclic lipopeptide with a sequence of GLDLVDDLL, was self-assembled on 1-dodecanthiol (DT) capped AuNPs (2.5 nm) (Figure 11(E,F)). Relative to the free SFT and DT-AuNPs, SFT/DT-AuNPs possessed the superior antimicrobial activity against several strains of bacteria and multi-drug resistance (MDR) bacteria (methicillin resistant *Staphylococcus aureus* (MRSA)). SFT/DT-AuNPs are effective in killing bacteria in MRSA infected wound in mice, promoting re-epithelialization and healing of wound [169]. It is observed that the lipid moiety attached to peptide helps AuNPs to penetrate effectively inside cells and bacteria. Likewise, DT-AuNPs modified with N-terminal fatty acrylated RWR/WRR peptides showed potent antimicrobial activity against a variety of microorganisms [170].

Microbial infection caused by medical devices is a major concern in the healthcare industry. In this context, we have immobilized the high density of CM peptide on AuNPs coated glass, titanium and polyurethane surfaces relative to other reports published previously [171,172]. These CM immobilized surfaces are potent to kill bacteria in the presence of human serum but do not induce platelet activation and cytotoxicity to human cells, demonstrating their potential in the development of medical devices with the antimicrobial property [171].

Stealth peptide-AuNP conjugates

The formation of protein corona around NPs elicits undesired cellular uptake, immune response and unavailability of conjugated biomolecules to interact with targets. The surface modifications of NPs with PEG, polysaccharides, mixed charged self-assembled and zwitterionic molecules are the most popular choices. Recently, an anti-fouling peptide composed of alternating negatively charge Glu (E) and positively charged Lys (K) amino acids has been discovered based on the

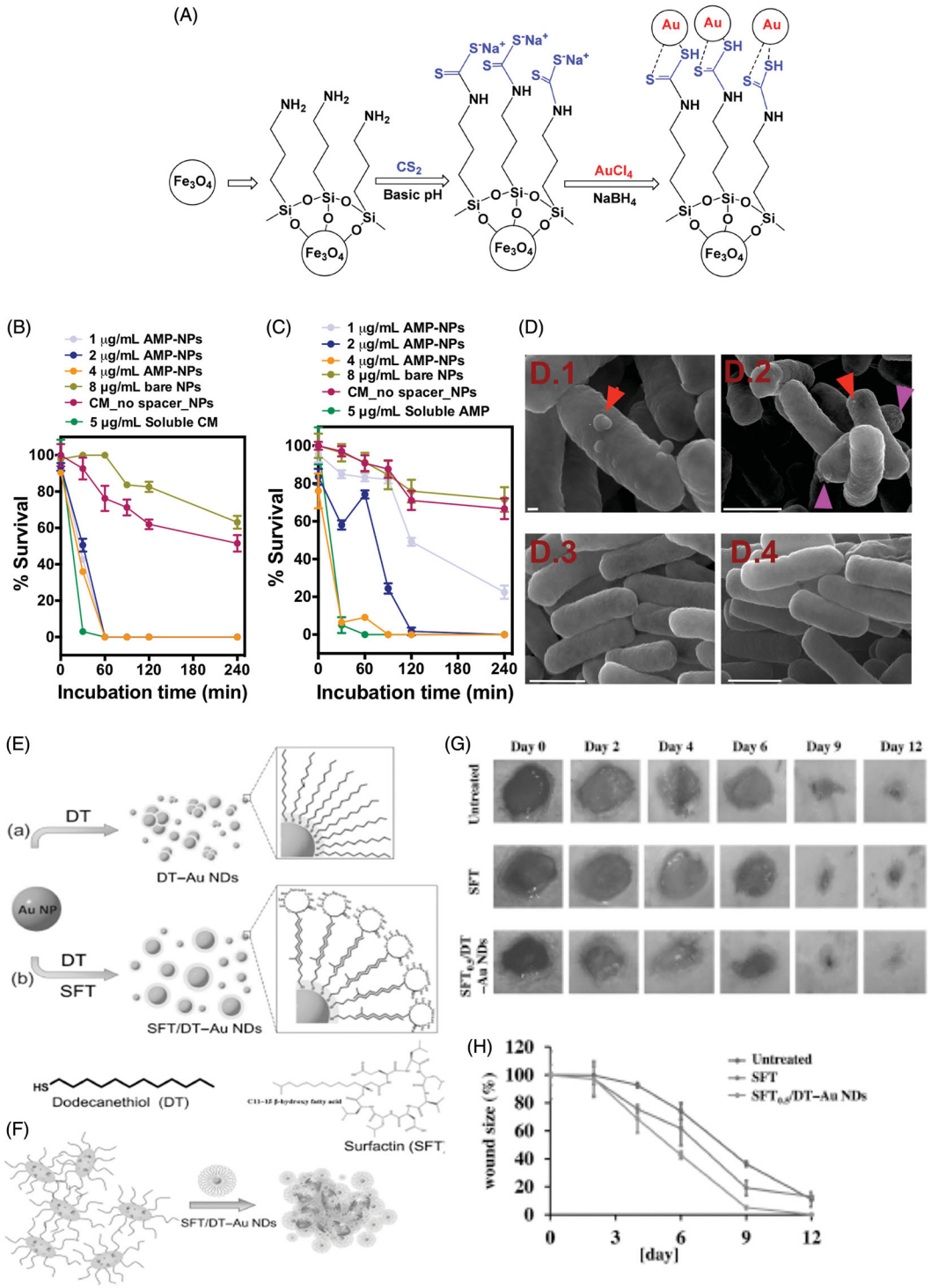

Figure 11. (A) Schematic diagram of CM-SH conjugation on SPION@Au core-shell NPs. Time course antimicrobial activity of 5 μg/mL of soluble CM (MIC of CM peptide) and different concentrations of AMP-NPs, bare NPs (8 μg/mL), and CM_no spacer_NPs (4 μg/mL) against 1×10^5 *E. coli* (B) or *S. aureus* (C). SEM images of *E. coli* treated with AMP-NP (4 μg/mL; D.1 and D.2) and bare NPs (8 μg/mL; D.3 and D.4) for 4 h. Red and purple arrows indicate blisters-like structures and protrusions of membrane, respectively. Scare bar for D.1 is 100 nm and for D.2 to D.4 is 1000 nm. (E) Synthesis of photoluminescent SFT/DT–Au NDs and (F) their antimicrobial activity through the SFT-mediated disruption of bacterial cells. (G) Representative photographs of the MRSA-infected wound untreated and treated with SFT or SFT/DT–Au NDs and (H) their corresponding wound sizes (relative area versus initial area). Error bars represent the standard deviation of three repeated measurements. Adopted from Maleki et al. [166] and Chen et al. [169].

analysis of over 1000 human proteins that have E and K amino acids on their surfaces [173,174]. The EK sequence of peptide forms a strong hydration layer around the surface similar to zwitterionic molecules, providing resistance to nonspecific protein adsorption [174]. Jiang's group developed a multifunctional stealth peptide sequence (EKEKEKE-PPPPCAm), consisting of a stealth EK sequence combined with a surface anchoring linker (4 Pro amino acids) and Cys amino acid (to interact with Au surface) [175]. The advantage of the Pro linker is that it forms a well-ordered structure with a high surface density, creating a robust self-assembled monolayer on the surface of NPs [176]. In this work, the authors modified the EK peptide with RGD sequence and showed high uptake of RGD-EK3-AuNPs by bovine aortic endothelial cells (Figure 12(A–C)) [175]. Recently, Wu *et al*. modified the EK peptide to CPPPPEKEKEK EKEKEDGR (HS-CPPP-EK5-RGD) peptide containing a CPPP anchoring linker and RGD sequence (Figure 12(D–F)) [177] and CGGGRRRRRRRRPLGLAGEKEKE KEKEKEKEKEKEK (HS-R8-PLGLAG-EK10) peptide [178] to selectively deliver the anticancer drug. Both peptides were conjugated to AuNPs to deliver 5-Aminolevulinic acid (ALA), the FDA-approved PDT precursor of PpIX that is hydrophilic and has low specificity to cancer cells. ALA was conjugated to AuNPs by a pH-responsive hydrazone bond that could be cleaved in the endolysosomal compartment of cells in an acidic environment. Both studies showed that the effective killing of cancer cells under the exposure of light (wavelength 635 nm) was due to generation of reactive oxygen species (ROS) as compared to the free ALA drugs (Figure 11(D–F)) [177,178].

Conclusion and perspectives

There have been rapid developments in the area of peptide conjugated AuNPs for various nanotechnology and biomedical applications in the last few years. In this review, we have discussed potential applications of peptide conjugated AuNPs in targeted drug/gene delivery, bioimaging, cancer therapy, brain targeting, immune modulation and antimicrobial materials, taking into account both *in vitro* and *in vivo* models. Importantly, the functional and structural versatility of peptides modulates the activity of peptide-AuNP conjugates, allowing them to be used in multifunctional manners. The easy surface functionalization, the oriented conjugation and the versatility of peptide chemistry makes peptide-AuNP conjugates attractive candidates in nanomedicine. The advantage with peptides is that they can be produced quickly in a cost-effective manner along with their easy modification with protease resistance residues, radio/fluorescent labels or reactive moieties *via* a solid-phase peptide synthesis approach. Despite several papers relating to the peptide-NP conjugates have been published globally, their clinical translations remain unsatisfactory, highlighting the challenges persist in nanomedicine fields. To tap the potential of peptide-AuNP conjugates as major players in nanomedicine, several issues must be considered and addressed carefully: (i) peptides may unfold during the contact with the surface of NPs due to various interactions (for instance electrostatic attraction, steric hindrance and heterogeneous complexation) exist between AuNPs and peptides, which ultimately influences their biological activities, delivery routes and applications. Although the formulation of peptide-NP conjugates is facile, rapid and scalable, the in-depth understanding of peptide conjugation events is still required to achieve promising biological properties in both *in vitro* and *in vivo* models. Molecular dynamic studies can provide such information to produce the optimum peptide-NP conjugates.

(ii) Importantly, the effect of protein corona on the biological properties of peptide-NP conjugates must also be studied to develop effective nanomedicines for clinical applications. Additionally, the composition of media or physiological solutions must be taken into consideration. Qualitative nanostructure-activity relationships (QNAR) understanding of protein corona-NPs may facilitate the generation of the optimal peptide-NP conjugates. Effective capping agents (for example PEG, stealth peptides, zwitterionic molecules) protect the peptide-NP conjugates from protein corona and provide stability and prolonged circulatory half-lives. The stability of peptide-NP conjugates determines their aggregation status, pharmacokinetics, biodistribution and systemic toxicity. Aggregation of peptide-NP conjugates in blood circulation leads to rapid clearance in liver and RES, reducing their probability to reach the targeted site (iii) Due to cellular environment complexity, appropriate peptide-NP conjugates must be developed to ensure the optimal activity in the organelle of cells without inducing any cytotoxicity. Quantitative structure-activity relationship (QSAR) study would be useful to design organelle-specific peptides by modifying its sequence. This study will help in expanding the library of peptides for cellular targeting. The combinatorial conjugation of the peptide cocktail on AuNPs will improve the delivery of cargos and biological performance such as membrane translocation property and the escape of peptide-NP conjugates from endosomes.

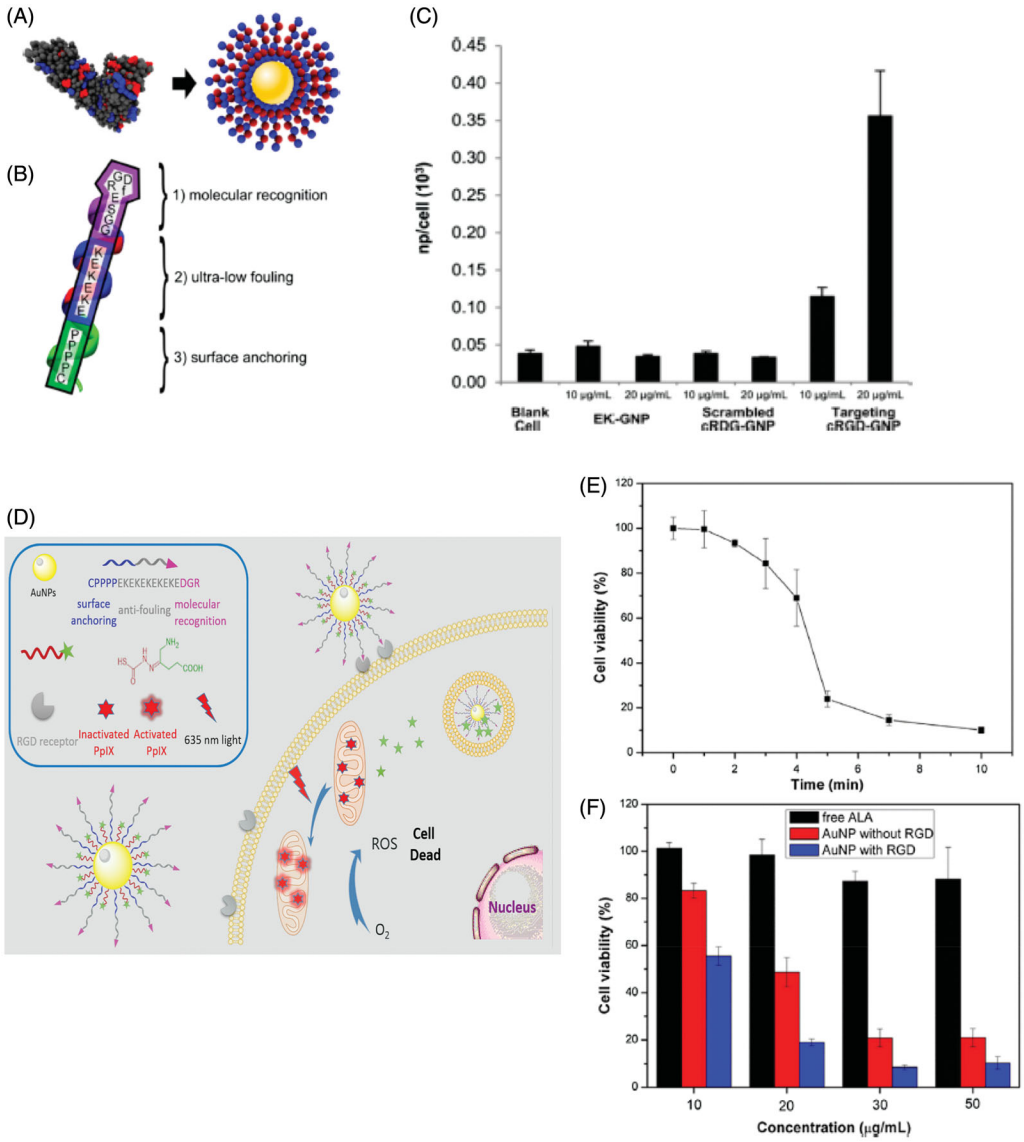

Figure 12. (A) Scheme depicting the design of the stealth peptide sequence inspired by the analysis of human protein surfaces, which contain E and K as the most prevalent amino acids on the surface (indicated by red and blue spheres). Structure of survivin-borealin-INCENP core complex (left). (B) All-in-one natural peptide sequence with three distinct functions: (1) biomolecular recognition *via* cyclic RGD (purple); (2) ultralow fouling *via* EK (red and blue); and (3) surface anchoring *via* PPPPC (green). (C) Cell uptake of EK-GNPs, scrambled cRDG-GNPs, and targeting cRGD-GNPs (number of gold nanoparticles per cell 10^3) in BAEC cells measured by ICP-MS. Each data point represents an average value ± standard deviation from at least three independent measurements. (D) Schematic illustration of ALA conjugated AuNPs for targeted PDT (E) A549 cell viability exposed to peptide protected ALA AuNPs with an equivalent ALA concentration of 50 μg/mL and irradiated for different time. (F) A549 cell viability exposed to different concentration of ALA in peptide protected ALA AuNPs with or without RGD respectively and irradiated with CW 635 nm light at 500 mW power. Adopted from Nowinski et al. [175] and Wu et al. [177].

Such findings will open new avenues for the targeted drug delivery applications.

(iv) Peptide-NP conjugates should be developed in such a way that there is enough room on the surface of NPs to load drugs without compromising the peptide activity. Modulating the density of peptides on AuNPs promotes the enhanced bioaccumulation and the activity of NPs in the targeted site of animal models. Therefore, suitable and standardized characterization of peptide-NP conjugates will improve our understanding of designing advanced NP conjugates. Currently, several papers related to peptide-NP conjugates have large discrepancies in results and interpretations. QNAR studies should be performed with great accuracy to meet clinical and regulatory standards. For example, the quantification of AuNPs in solution or the conjugated peptide

on the surface of AuNPs often varies in the literature due to the inherent complexity of peptide-NP conjugates. (v) There is a need to develop universal tools and protocols to determine the long-term cytotoxicity and bioactivity of different peptide-NP conjugates. Such studies will provide a library of information that can be useful in drawing reliable cytotoxicity and biological properties of peptide-NP conjugates. Novel and advanced characterization tools such as high-throughput screening and high-resolution microscopy start to emerge in the market that can solve these issues.

It is reasonable to believe that, in future, several peptides either derived from the natural proteins or the molecular dynamics study would be discovered to design the complexed peptide-NP conjugates for efficient targeting, immunotherapy and delivery of drugs in patient's body based on the initial lessons learned from *in vitro* and *in vivo* models. Consequently, our ability to diagnose and treat different life-threatening diseases will be improved, which in turn reduces the huge healthcare costs from society.

Disclosure statement

No potential conflict of interest was reported by the author(s).

Funding

AR would like to thank the investigator program (IF/00539/2015) and UIDB/04539/2020 project through Compete 2020 and FCT (Fundação para a Ciência e a Tecnologia).

References

[1] Elahi N, Kamali M, Baghersad MH. Recent biomedical applications of gold nanoparticles: a review. Talanta. 2018; 184:537–556.
[2] Daraee H, Eatemadi A, Abbasi E, et al. Application of gold nanoparticles in biomedical and drug delivery. Artif Cells Nanomed Biotechnol. 2016;44(1):410–422.
[3] Dykman L, Khlebtsov N. Gold nanoparticles in biomedical applications: recent advances and perspectives. Chem Soc Rev. 2012;41(6):2256–2282.
[4] Dykman LA, Khlebtsov NG. Gold Nanoparticles in biology and medicine: recent advances and prospects. Acta Naturae. 2011;3(2):34–55.
[5] Jeong H-H, Choi E, Ellis E, et al. Recent advances in gold nanoparticles for biomedical applications: from hybrid structures to multi-functionality. J Mater Chem B. 2019;7(22):3480–3496.
[6] Zhang J, Mou L, Jiang X. Surface chemistry of gold nanoparticles for health-related applications. Chem Sci. 2020;11(4):923–936.
[7] Mieszawska AJ, Mulder WJM, Fayad ZA, et al. Multifunctional gold nanoparticles for diagnosis and therapy of disease. Mol Pharmaceutics. 2013;10(3): 831–847.
[8] Mahato K, Nagpal S, Shah MA, et al. Gold nanoparticle surface engineering strategies and their applications in biomedicine and diagnostics. 3 Biotech. 2019;9(2):57
[9] Henninot A, Collins JC, Nuss JM. The current state of peptide drug discovery: back to the future? J Med Chem. 2018;61(4):1382–1414.
[10] Farhadi T, Hashemian SM. Computer-aided design of amino acid-based therapeutics: a review. Drug Des Devel Ther. 2018;12:1239–1254.
[11] Bozovicar K, Bratkovic T. Evolving a peptide: library platforms and diversification strategies. Int J Mol Sci. 2020;21(1):215.
[12] Hou W, Zhang X, Liu C-F. Progress in chemical synthesis of peptides and proteins. Trans Tianjin Univ. 2017;23(5):401–419.
[13] Jeong WJ, Bu J, Kubiatowicz LJ, et al. Peptide-nanoparticle conjugates: a next generation of diagnostic and therapeutic platforms? Nano Converg. 2018;5(1):38.
[14] Lau JL, Dunn MK. Therapeutic peptides: historical perspectives, current development trends, and future directions. Bioorgan Med Chem. 2018;26(10): 2700–2707.
[15] Koo HB, Seo J. Antimicrobial peptides under clinical investigation. Peptide Sci. 2019;111:e24122.
[16] Divyashree M, Mani MK, Reddy D, et al. Clinical applications of antimicrobial peptides (AMPs): where do we stand now? Protein Pept Lett. 2020;27(2): 120–134.
[17] Monti S, Barcaro G, Sementa L, et al. Dynamics and self-assembly of bio-functionalized gold nanoparticles in solution: reactive molecular dynamics simulations. Nano Res. 2018;11(4):1757–1767.
[18] Walsh TR, Knecht MR. Biointerface structural effects on the properties and applications of bioinspired peptide-based nanomaterials. Chem Rev. 2017; 117(20):12641–12704.
[19] Bastus NG, Sanchez-Tillo E, Pujals S, et al. Peptides conjugated to gold nanoparticles induce macrophage activation. Mol Immunol. 2009;46:743–748.
[20] Bastus NG, Sanchez-Tillo E, Pujals S, et al. Homogeneous conjugation of peptides onto gold nanoparticles enhances macrophage response. ACS Nano. 2009;3(6):1335–1344.
[21] Gessner I, Klimpel A, Klußmann M, et al. Interdependence of charge and secondary structure on cellular uptake of cell penetrating peptide functionalized silica nanoparticles. Nanoscale Adv. 2020; 2(1):453–462.
[22] Spicer CD, Jumeaux C, Gupta B, et al. Peptide and protein nanoparticle conjugates: versatile platforms for biomedical applications. Chem Soc Rev. 2018; 47(10):3574–3620.
[23] Yang WT, Guo WS, Chang J, et al. Protein/peptide-templated biomimetic synthesis of inorganic nanoparticles for biomedical applications. J Mater Chem B. 2017;5(3):401–417.

[24] Zong JY, Cobb SL, Cameron NR. Peptide-functionalized gold nanoparticles: versatile biomaterials for diagnostic and therapeutic applications. Biomater Sci. 2017;5(5):872–886.
[25] Liu X, Zhang Q, Knoll W, et al. Rational design of functional peptide-gold hybrid nanomaterials for molecular interactions. Adv Mater. 2020;32(37): 2000866.
[26] Egorova EA, van Rijt MMJ, Sommerdijk N, et al. One peptide for them all: gold nanoparticles of different sizes are stabilized by a common peptide amphiphile. ACS Nano. 2020;14(5):5874–5886.
[27] Govorov AO, Gun'ko YK, Slocik JM, et al. Chiral nanoparticle assemblies: circular dichroism, plasmonic interactions, and exciton effects. J Mater Chem. 2011; 21(42):16806–16818.
[28] Slocik JM, Govorov AO, Naik RR. Plasmonic circular dichroism of peptide-functionalized gold nanoparticles. Nano Lett. 2011;11(2):701–705.
[29] Boisselier E, Astruc D. Gold nanoparticles in nanomedicine: preparations, imaging, diagnostics, therapies and toxicity. Chem Soc Rev. 2009;38(6):1759–1782.
[30] Zhang DL, Luo G, Ding XX, et al. Preclinical experimental models of drug metabolism and disposition in drug discovery and development. Acta Pharm Sin B. 2012;2(6):549–561.
[31] Kalepu S, Nekkanti V. Insoluble drug delivery strategies: review of recent advances and business prospects. Acta Pharm Sin B. 2015;5(5):442–453.
[32] Li T, He XX, Wang ZX. The application of peptide functionalized gold nanoparticles. ACS Sym Ser. 2012;1113:55–68.
[33] Chen WH, Luo GF, Zhang XZ. Recent advances in subcellular targeted cancer therapy based on functional materials. Adv Mater. 2019;31(3):1802725.
[34] Wang J, Hu X, Xiang D. Nanoparticle drug delivery systems: an excellent carrier for tumor peptide vaccines. Drug Deliv. 2018;25(1):1319–1327.
[35] Kodiha M, Wang YM, Hutter E, et al. Off to the organelles - killing cancer cells with targeted gold nanoparticles. Theranostics. 2015;5(4):357–370.
[36] Mieszawska AJ, Mulder WJ, Fayad ZA, et al. Multifunctional gold nanoparticles for diagnosis and therapy of disease. Mol Pharm. 2013;10(3):831–847.
[37] Chen YP, Xianyu YL, Jiang XY. Surface modification of gold nanoparticles with small molecules for biochemical analysis. Acc Chem Res. 2017;50(2):310–319.
[38] Bartczak D, Nitti S, Millar TM, et al. Exocytosis of peptide functionalized gold nanoparticles in endothelial cells. Nanoscale. 2012;4(15):4470–4472.
[39] Pujals S, Sabido E, Tarrago T, et al. All-D proline-rich cell-penetrating peptides: a preliminary in vivo internalization study. Biochem Soc T. 2007;35(4): 794–796.
[40] Pujals S, Bastus NG, Pereiro E, et al. Shuttling gold nanoparticles into tumoral cells with an amphipathic proline-rich peptide. Chembiochem. 2009;10(6): 1025–1031.
[41] Krpetic Z, Saleemi S, Prior IA, et al. Negotiation of intracellular membrane barriers by TAT-modified gold nanoparticles. ACS Nano. 2011;5(6):5195–5201.
[42] Nativo P, Prior IA, Brust M. Uptake and intracellular fate of surface-modified gold nanoparticles. ACS Nano. 2008;2(8):1639–1644.
[43] Petersen S, Barchanski A, Taylor U, et al. Penetratin-conjugated gold nanoparticles - design of cell-penetrating nanomarkers by femtosecond laser ablation. J Phys Chem C. 2011;115(12):5152–5159.
[44] Tiwari PM, Eroglu E, Bawage SS, et al. Enhanced intracellular translocation and biodistribution of gold nanoparticles functionalized with a cell-penetrating peptide (VG-21) from vesicular stomatitis virus. Biomaterials. 2014;35(35):9484–9494.
[45] Lee JS, Tung CH. Enhancing the cellular delivery of nanoparticles using lipo-oligoarginine peptides. Adv Funct Mater. 2012;22(23):4924–4930.
[46] Singh L, Parboosing R, Kruger HG, et al. Intracellular localization of gold nanoparticles with targeted delivery in MT-4 lymphocytes. Adv Nat Sci: Nanosci Nanotechnol. 2016;7(4):045013.
[47] Tkachenko AG, Xie H, Liu YL, et al. Cellular trajectories of peptide-modified gold particle complexes: Comparison of nuclear localization signals and peptide transduction domains. Bioconjug Chem. 2004; 15(3):482–490.
[48] Wei L, Yang QY, Xiao LH. Tempo-spatially resolved cellular dynamics of human immunodeficiency virus transacting activator of transcription (Tat) peptide-modified nanocargos in living cells. Nanoscale. 2014; 6(17):10207–10215.
[49] Yang C, Uertz J, Yohan D, et al. Peptide modified gold nanoparticles for improved cellular uptake, nuclear transport, and intracellular retention. Nanoscale. 2014;6(20):12026–12033.
[50] Ye S, Kang N, Chen M, et al. Tat/HA2 peptides conjugated AuNR@pNIPAAm as a photosensitizer carrier for near infrared triggered photodynamic therapy. Mol Pharm. 2015;12(7):2444–2458.
[51] Cesbron Y, Shaheen U, Free P, et al. TAT and HA2 facilitate cellular uptake of gold nanoparticles but do not lead to cytosolic localisation. Plos One. 2015; 10(4):e0121683.
[52] Oliveira S, van Rooy I, Kranenburg O, et al. Fusogenic peptides enhance endosomal escape improving siRNA-induced silencing of oncogenes. Int J Pharm. 2007;331(2):211–214.
[53] Wang GK, Norton AS, Pokharel D, et al. KDEL peptide gold nanoconstructs: promising nanoplatforms for drug delivery. Nanomedicine. 2013;9(3):366–374.
[54] Oh E, Delehanty JB, Sapsford KE, et al. Cellular uptake and fate of PEGylated gold nanoparticles is dependent on both cell-penetration peptides and particle size. ACS Nano. 2011;5(8):6434–6448.
[55] Sun LL, Liu DJ, Wang ZX. Functional gold nanoparticle-peptide complexes as cell-targeting agents. Langmuir. 2008;24(18):10293–10297.
[56] Todorova N, Chiappini C, Mager M, et al. Surface presentation of functional peptides in solution determines cell internalization efficiency of TAT conjugated nanoparticles. Nano Lett. 2014;14(9): 5229–5237.
[57] Santi M, Maccari G, Mereghetti P, et al. Rational design of a transferrin-binding peptide sequence

tailored to targeted nanoparticle internalization. Bioconjug Chem. 2017;28(2):471–480.
[58] Wang GK, Papasani MR, Cheguru P, et al. Gold-peptide nanoconjugate cellular uptake is modulated by serum proteins. Nanomed-Nanotechnol. 2012;8(6):822–832.
[59] Albanese A, Chan WCW. Effect of gold nanoparticle aggregation on cell uptake and toxicity. ACS Nano. 2011;5(7):5478–5489.
[60] Ojea-Jimenez I, Garcia-Fernandez L, Lorenzo J, et al. Facile preparation of cationic gold nanoparticle-bioconjugates for cell penetration and nuclear targeting. ACS Nano. 2012;6(9):7692–7702.
[61] Thakor AS, Jokerst J, Zavaleta C, et al. Gold Nanoparticles: a revival in precious metal administration to patients. Nano Lett. 2011;11(10):4029–4036.
[62] Chen WH, Chen JX, Cheng H, et al. A new anti-cancer strategy of damaging mitochondria by pro-apoptotic peptide functionalized gold nanoparticles. Chem Commun (Camb). 2013;49(57):6403–6405.
[63] Ma XC, Wang XB, Zhou M, et al. A mitochondria-targeting gold-peptide nanoassembly for enhanced cancer-cell killing. Adv Healthc Mater. 2013;2(12):1638–1643.
[64] Akrami M, Balalaie S, Hosseinkhani S, et al. Tuning the anticancer activity of a novel pro-apoptotic peptide using gold nanoparticle platforms. Sci Rep. 2016;6:31030.
[65] Galbiati E, Gambini L, Civitarese V, et al. "Blind" targeting in action: from phage display to breast cancer cell targeting with peptide-gold nanoconjugates. Pharmacol Res. 2016;111:155–162.
[66] Jimenez-Mancilla N, Ferro-Flores G, Ocampo-Garcia B, et al. Multifunctional targeted radiotherapy system for induced tumours expressing gastrin-releasing peptide receptors. CNANO. 2012;8(2):193–201.
[67] Vilchis-Juarez A, Ferro-Flores G, Santos-Cuevas C, et al. Molecular targeting radiotherapy with cyclo-RGDfK(C) peptides conjugated to Lu-177-labeled gold nanoparticles in tumor-bearing mice. J. Biomed. Nanotechnol. 2014;10:393–404.
[68] Li YJ, Zhao LZ, Xu XY, et al. Design of Tc-99(m)-labeled low generation dendrimer-entrapped gold nanoparticles for targeted single photon emission computed tomography/computed tomography imaging of gliomas. J Biomed Nanotechnol. 2019;15(6):1201–1212.
[69] Antosh MP, Wijesinghe DD, Shrestha S, et al. Enhancement of radiation effect on cancer cells by gold-pHLIP. Proc Natl Acad Sci U S A. 2015;112(17):5372–5376.
[70] Yao L, Danniels J, Moshnikova A, et al. pHLIP peptide targets nanogold particles to tumors. Proc Natl Acad Sci U S A. 2013;110(2):465–470.
[71] Qu XC, Li XX, Liang JN, et al. Micro-CT Imaging of RGD-conjugated gold nanorods targeting tumor in vivo. J. Nanomater. 2016;2016:1–13.
[72] Wu MH, Zhang YY, Zhang Y, et al. Tumor angiogenesis targeting and imaging using gold nanoparticle probe with directly conjugated cyclic NGR. RSC Adv. 2018;8(3):1706–1716.
[73] Sun MM, Peng D, Hao HJ, et al. Thermally triggered in situ assembly of gold nanoparticles for cancer multimodal imaging and photothermal therapy. ACS Appl Mater Interfaces. 2017;9(12):10453–10460.
[74] Zhang L, Su HL, Cai JL, et al. A multifunctional platform for tumor angiogenesis-targeted chemo-thermal therapy using polydopamine-coated gold nanorods. ACS Nano. 2016;10(11):10404–10417.
[75] Chen Q, Wang H, Liu H, et al. Multifunctional dendrimer-entrapped gold nanoparticles modified with RGD peptide for targeted computed tomography/magnetic resonance dual-modal imaging of tumors. Anal Chem. 2015;87(7):3949–3956.
[76] Zhao Y, Liu W, Tian Y, et al. Anti-EGFR peptide-conjugated triangular gold nanoplates for computed tomography/photoacoustic imaging-guided photothermal therapy of non-small cell lung cancer. ACS Appl Mater Interfaces. 2018;10(20):16992–17003.
[77] Lee SB, Lee YJ, Cho SJ, et al. Antigen-free radionuclide-embedded gold nanoparticles for dendritic cell maturation, tracking, and strong antitumor immunity. Adv Healthc Mater. 2018;7:e170369.
[78] Kumar A, Ma HL, Zhang X, et al. Gold nanoparticles functionalized with therapeutic and targeted peptides for cancer treatment. Biomaterials. 2012;33(4):1180–1189.
[79] Kumar A, Huo SD, Zhang X, et al. Neuropilin-1-targeted gold nanoparticles enhance therapeutic efficacy of platinum(IV) drug for prostate cancer treatment. ACS Nano. 2014;8(5):4205–4220.
[80] Ali MRK, Wu Y, Ghosh D, et al. Nuclear membrane-targeted gold nanoparticles inhibit cancer cell migration and invasion. ACS Nano. 2017;11(4):3716–3726.
[81] Alkilany AM, Boulos SP, Lohse SE, et al. Homing peptide-conjugated gold nanorods: the effect of amino acid sequence display on nanorod uptake and cellular proliferation. Bioconjugate Chem. 2014;25(6):1162–1171.
[82] Chanda N, Shukla R, Katti KV, et al. Gastrin releasing protein receptor specific gold nanorods: breast and prostate tumor avid nanovectors for molecular imaging. Nano Lett. 2009;9(5):1798–1805.
[83] Heidari Z, Sariri R, Salouti M. Gold nanorods-bombesin conjugate as a potential targeted imaging agent for detection of breast cancer. J Photochem Photobio B. 2014;130:40–46.
[84] Chanda N, Kattumuri V, Shukla R, et al. Bombesin functionalized gold nanoparticles show in vitro and in vivo cancer receptor specificity. Proc Natl Acad Sci U S A. 2010;107(19):8760–8765.
[85] Avvakumova S, Galbiati E, Pandolfi L, et al. Development of U11-functionalized gold nanoparticles for selective targeting of urokinase plasminogen activator receptor-positive breast cancer cells. Bioconjug Chem. 2014;25(8):1381–1386.
[86] Huang XH, Peng XH, Wang YQ, et al. A reexamination of active and passive tumor targeting by using rod-shaped gold nanocrystals and covalently conjugated peptide ligands (vol 4, pg 5887, 2010). ACS Nano. 2011;5(8):6765–6765.
[87] Hosta-Rigau L, Olmedo I, Arbiol J, et al. Multifunctionalized gold nanoparticles with peptides

targeted to gastrin-releasing peptide receptor of a tumor cell line. Bioconjug Chem. 2010;21(6): 1070–1078.
[88] Huang XH, Peng XH, Wang YQ, et al. A reexamination of active and passive tumor targeting by using rod-shaped gold nanocrystals and covalently conjugated peptide ligands. ACS Nano. 2010;4(10): 5887–5896.
[89] Jha S, Ramadori F, Quarta S, et al. Binding and uptake into human hepatocellular carcinoma cells of peptide-functionalized gold nanoparticles. Bioconjug Chem. 2017;28(1):222–229.
[90] Poon W, Zhang X, Bekah D, et al. Targeting B16 tumors in vivo with peptide-conjugated gold nanoparticles. Nanotechnology. 2015;26(28):285101.
[91] Park H, Tsutsumi H, Mihara H. Cell penetration and cell-selective drug delivery using α-helix peptides conjugated with gold nanoparticles . Biomaterials. 2013;34(20):4872–4879.
[92] Park H, Tsutsumi H, Mihara H. Cell-selective intracellular drug delivery using doxorubicin and α-helical peptides conjugated to gold nanoparticles. Biomaterials. 2014;35(10):3480–3487.
[93] Chen GC, Xie YS, Peltier R, et al. Peptide-decorated gold nanoparticles as functional nano-capping agent of mesoporous silica container for targeting drug delivery. ACS Appl Mater Interfaces. 2016;8(18): 11204–11209.
[94] See V, Free P, Cesbron Y, et al. Cathepsin L digestion of nanobioconjugates upon endocytosis. ACS Nano. 2009;3(9):2461–2468.
[95] Parween S, Ali A, Chauhan VS. Non-natural amino acids containing peptide-capped gold nanoparticles for drug delivery application. ACS Appl Mater Interfaces. 2013;5(14):6484–6493.
[96] Kalimuthu K, Lubin BC, Bazylevich A, et al. Gold nanoparticles stabilize peptide-drug-conjugates for sustained targeted drug delivery to cancer cells. J. Nanobiotechnol. 2018;16:34.
[97] Hou Z, Wang Z, Liu R, et al. The effect of phosphopeptide on the stability of gold nanoparticles and drug delivery. J Nanobiotechnology. 2019;17(1):88.
[98] Bartczak D, Muskens OL, Sanchez-Elsner T, et al. Manipulation of in vitro angiogenesis using peptide-coated gold nanoparticles. ACS Nano. 2013;7(6): 5628–5636.
[99] Bartczak D, Muskens OL, Nitti S, et al. Nanoparticles for inhibition of in vitro tumour angiogenesis: synergistic actions of ligand function and laser irradiation. Biomater Sci. 2015;3(5):733–741.
[100] Gobin AM, Moon JJ, West JL. EphrinA1-targeted nanoshells for photothermal ablation of prostate cancer cells. Int J Nanomed. 2008;3:351–358.
[101] Heidari Z, Salouti M, Sariri R. Breast cancer photothermal therapy based on gold nanorods targeted by covalently-coupled bombesin peptide. Nanotechnology. 2015;26(19):195101.
[102] Tan HX, Huang YZ, Xu JH, et al. Spider toxin peptide lycosin-I functionalized gold nanoparticles for in vivo tumor targeting and therapy. Theranostics. 2017; 7(12):3168–3178.
[103] Patino T, Mahajan U, Palankar R, et al. Multifunctional gold nanorods for selective plasmonic photothermal therapy in pancreatic cancer cells using ultra-short pulse near-infrared laser irradiation. Nanoscale. 2015;7(12):5328–5337.
[104] Li X, Xing LX, Hu Y, et al. An RGD-modified hollow silica@Au core/shell nanoplatform for tumor combination therapy. Acta Biomater. 2017; 62:273–283.
[105] Ali MRK, Wu Y, Tang Y, et al. Targeting cancer cell integrins using gold nanorods in photothermal therapy inhibits migration through affecting cytoskeletal proteins. Proc Natl Acad Sci U S A. 2017;114(28): E5655–E5663.
[106] Qiu WX, Liu LH, Li SY, et al. ACPI conjugated gold nanorods as nanoplatform for dual image guided activatable photodynamic and photothermal combined therapy in vivo. Small. 2017;13(18):1603956.
[107] Meyers JD, Cheng Y, Broome AM, et al. Peptide-targeted gold nanoparticles for photodynamic therapy of brain cancer. Part Part Syst Charact. 2015;32(4): 448–457.
[108] Wu L, Xu F, Reinhard BM. Nanoconjugation prolongs endosomal signaling of the epidermal growth factor receptor and enhances apoptosis. Nanoscale. 2016; 8(28):13755–13768.
[109] Wang NN, Zhao ZL, Lv YF, et al. Gold nanorod-photosensitizer conjugate with extracellular pH-driven tumor targeting ability for photothermal/photodynamic therapy. Nano Res. 2014;7(9):1291–1301.
[110] Oh MH, Yu JH, Kim I, et al. Genetically programmed clusters of gold nanoparticles for cancer cell-targeted photothermal therapy. ACS Appl Mater Interfaces. 2015;7(40):22578–22586.
[111] Pedrosa P, Heuer-Jungemann A, Kanaras AG, et al. Potentiating angiogenesis arrest in vivo via laser irradiation of peptide functionalised gold nanoparticles. J. Nanobiotechnol. 2017;15:85.
[112] Roma-Rodrigues C, Heuer-Jungemann A, Fernandes AR, et al. Peptide-coated gold nanoparticles for modulation of angiogenesis in vivo. Int. J. Nanomed. 2016;11:2633–2639.
[113] Gormley AJ, Malugin A, Ray A, et al. Biological evaluation of RGDfK-gold nanorod conjugates for prostate cancer treatment. J Drug Target. 2011;19(10): 915–924.
[114] Silva F, Zambre A, Campello MPC, et al. Interrogating the role of receptor-mediated mechanisms: biological fate of peptide-functionalized radiolabeled gold nanoparticles in tumor mice. Bioconjug Chem. 2016; 27(4):1153–1164.
[115] Yang Y, Zhang L, Cai JL, et al. Tumor angiogenesis targeted radiosensitization therapy using gold nanoprobes guided by MRI/SPECT imaging. ACS Appl Mater Interfaces. 2016;8(3):1718–1732.
[116] Guerrero S, Araya E, Fiedler JL, et al. Improving the brain delivery of gold nanoparticles by conjugation with an amphipathic peptide. Nanomedicine (Lond). 2010;5(6):897–913.
[117] Guerrero S, Herance JR, Rojas S, et al. Synthesis and in vivo evaluation of the biodistribution of a F-18-labeled conjugate gold-nanoparticle-peptide with

potential biomedical application. Bioconjugate Chem. 2012;23(3):399–408.
[118] Prades R, Guerrero S, Araya E, et al. Delivery of gold nanoparticles to the brain by conjugation with a peptide that recognizes the transferrin receptor. Biomaterials. 2012;33(29):7194–7205.
[119] Oller-Salvia B, Sanchez-Navarro M, Ciudad S, et al. MiniAp-4: a venom-inspired peptidomimetic for brain delivery. Angew Chem Int Ed Engl. 2016;55(2): 572–575.
[120] Lee JH, Engler JA, Collawn JF, et al. Receptor mediated uptake of peptides that bind the human transferrin receptor. Eur J Biochem. 2001;268(7): 2004–2012.
[121] Praca C, Rai A, Santos T, et al. A nanoformulation for the preferential accumulation in adult neurogenic niches. J Control Release. 2018;284:57–72.
[122] Ruff J, Hüwel S, Kogan MJ, et al. The effects of gold nanoparticles functionalized with ß-amyloid specific peptides on an in vitro model of blood-brain barrier. Nanomedicine. 2017;13(5):1645–1652.
[123] Albertini B, Mathieu V, Iraci N, et al. Tumor targeting by peptide-decorated gold nanoparticles. Mol Pharm. 2019;16(6):2430–2444.
[124] Xu XY, Liu K, Wang Y, et al. A multifunctional low-generation dendrimer-based nanoprobe for the targeted dual mode MR/CT imaging of orthotopic brain gliomas. J Mater Chem B. 2019;7(23):3639–3643.
[125] Frigell J, Garcia I, Gomez-Vallejo V, et al. Ga-68-labeled gold glyconanoparticles for exploring blood-brain barrier permeability: preparation, biodistribution studies, and improved brain uptake via neuropeptide conjugation. J Am Chem Soc. 2014; 136(1):449–457.
[126] Cheng Y, Meyers JD, Agnes RS, et al. Addressing brain tumors with targeted gold nanoparticles: a new gold standard for hydrophobic drug delivery? Small. 2011;7(16):2301–2306.
[127] Dixit S, Novak T, Miller K, et al. Transferrin receptor-targeted theranostic gold nanoparticles for photosensitizer delivery in brain tumors. Nanoscale. 2015; 7(5):1782–1790.
[128] Cheng Y, Dai Q, Morshed RA, et al. Blood-brain barrier permeable gold nanoparticles: an efficient delivery platform for enhanced malignant glioma therapy and imaging. Small. 2014;10(24):5137–5150.
[129] Morshed RA, Muroski ME, Dai Q, et al. Cell-penetrating peptide-modified gold nanoparticles for the delivery of doxorubicin to brain metastatic breast cancer. Mol Pharm. 2016;13(6):1843–1854.
[130] Lu W, Melancon MP, Xiong CY, et al. Effects of photoacoustic imaging and photothermal ablation therapy mediated by targeted hollow gold nanospheres in an orthotopic mouse xenograft model of glioma. Cancer Res. 2011;71(19):6116–6121.
[131] Kogan MJ, Bastus NG, Amigo R, et al. Nanoparticle-mediated local and remote manipulation of protein aggregation. Nano Lett. 2006;6(1):110–115.
[132] Araya E, Olmedo I, Bastus NG, et al. Gold nanoparticles and microwave irradiation inhibit beta-amyloid amyloidogenesis. Nanoscale Res Lett. 2008;3(11): 435–443.
[133] Olmedo I, Araya E, Sanz F, et al. How changes in the sequence of the peptide CLPFFD-NH2 can modify the conjugation and stability of gold nanoparticles and their affinity for beta-amyloid fibrils. Bioconjugate Chem. 2008;19(6):1154–1163.
[134] Xiong N, Zhao YJ, Dong XY, et al. Design of a molecular hybrid of dual peptide inhibitors coupled on aunps for enhanced inhibition of amyloid beta-protein aggregation and cytotoxicity. Small. 2017; 13(13):1601666.
[135] Yin TT, Xie WJ, Sun J, et al. Penetratin peptide-functionalized gold nanostars: enhanced BBB Permeability and NIR photothermal treatment of Alzheimer's disease using ultralow irradiance. ACS Appl Mater Interfaces. 2016;8(30):19291–19302.
[136] Ruff J, Hassan N, Morales-Zavala F, et al. CLPFFD-PEG functionalized NIR-absorbing hollow gold nanospheres and gold nanorods inhibit β-amyloid aggregation . J Mater Chem B. 2018;6(16):2432–2443.
[137] Li M, Guan Y, Zhao A, et al. Using multifunctional peptide conjugated Au nanorods for monitoring β-amyloid aggregation and chemo-photothermal treatment of Alzheimer's disease. Theranostics. 2017; 7(12):2996–3006.
[138] Yang H, Fung SY, Xu S, et al. Amino acid-dependent attenuation of toll-like receptor signaling by peptide-gold nanoparticle hybrids. ACS Nano. 2015;9(7): 6774–6784.
[139] Yang H, Zhou YZ, Fung SY, et al. Amino acid structure determines the immune responses generated by peptide-gold nanoparticle hybrids. Part Part Syst Charact. 2013;30(12):1039–1043.
[140] Yang H, Kozicky L, Saferali A, et al. Endosomal pH modulation by peptide-gold nanoparticle hybrids enables potent anti-inflammatory activity in phagocytic immune cells. Biomaterials. 2016;111:90–102.
[141] Cruz LJ, Rueda F, Cordobilla B, et al. Targeting nanosystems to human DCs via Fc receptor as an effective strategy to deliver antigen for immunotherapy. Mol Pharm. 2011;8(1):104–116.
[142] Mocan T, Matea C, Tabaran F, et al. in vitro administration of gold nanoparticles functionalized with MUC-1 protein fragment generates anticancer vaccine response via macrophage activation and polarization mechanism. J Cancer. 2015;6(6):583–592.
[143] Cai H, Degliangeli F, Palitzsch B, et al. Glycopeptide-functionalized gold nanoparticles for antibody induction against the tumor associated mucin-1 glycoprotein. Bioorgan Med Chem. 2016;24(5): 1132–1135.
[144] Almeida JPM, Lin AY, Figueroa ER, et al. In vivo gold nanoparticle delivery of peptide vaccine induces anti-tumor immune response in prophylactic and therapeutic tumor models. Small. 2015;11(12): 1453–1459.
[145] Lin AY, Lunsford J, Bear AS, et al. High-density sub-100-nm peptide-gold nanoparticle complexes improve vaccine presentation by dendritic cells in vitro. Nanoscale Res Lett. 2013;8(1):72.
[146] Cheung WH, Chan VSF, Pang HW, et al. Conjugation of latent membrane protein (LMP)-2 epitope to gold nanoparticles as highly immunogenic multiple

antigenic peptides for induction of Epstein-Barr virus-specific cytotoxic T-lymphocyte responses in vitro. Bioconjug Chem. 2009;20(1):24–31.
[147] Chen YS, Hung YC, Lin WH, et al. Assessment of gold nanoparticles as a size-dependent vaccine carrier for enhancing the antibody response against synthetic foot-and-mouth disease virus peptide. Nanotechnology. 2010;21(19):195101.
[148] Lee CH, Syu SH, Chen YS, et al. Gold nanoparticles regulate the blimp1/pax5 pathway and enhance antibody secretion in B-cells. Nanotechnology. 2014; 25(12):125103.
[149] Di Gianvincenzo P, Calvo J, Perez S, et al. Negatively charged glyconanoparticles modulate and stabilize the secondary structures of a gp120 V3 loop peptide: toward fully synthetic HIV vaccine candidates. Bioconjugate Chem. 2015;26(4):755–765.
[150] Zhou QQ, Zhang YL, Du J, et al. Different-sized gold nanoparticle activator/antigen increases dendritic cells accumulation in liver-draining lymph nodes and CD8+ T cell responses. ACS Nano. 2016;10(2): 2678–2692.
[151] Safari D, Marradi M, Chiodo F, et al. Gold nanoparticles as carriers for a synthetic Streptococcus pneumoniae type 14 conjugate vaccine. Nanomedicine (Lond). 2012;7(5):651–1112.
[152] Dakterzada F, Mobarez AM, Roudkenar MH, et al. Induction of humoral immune response against Pseudomonas aeruginosa flagellin(1-161) using gold nanoparticles as an adjuvant. Vaccine. 2016;34(12): 1472–1479.
[153] Patel PC, Giljohann DA, Seferos DS, et al. Peptide antisense nanoparticles. Proc Natl Acad Sci U S A. 2008;105(45):17222–17226.
[154] Acharya S, Hill RA. High efficacy gold-KDEL peptide-siRNA nanoconstruct-mediated transfection in C2C12 myoblasts and myotubes. Nanomed.-Nanotechnol. 2014;10(2):329–337.
[155] Sun TM, Simmons R, Huo D, et al. Targeted delivery of anti-miR-712 by VCAM1-binding Au nanospheres for atherosclerosis therapy. ChemNanoMat. 2016;2(5): 400–406.
[156] Muroski ME, Morgan TJ, Levenson CW, et al. A gold nanoparticle pentapeptide: gene fusion to induce therapeutic gene expression in mesenchymal stem cells. J Am Chem Soc. 2014;136(42):14763–14771.
[157] Peng LH, Huang YF, Zhang CZ, et al. Integration of antimicrobial peptides with gold nanoparticles as unique non-viral vectors for gene delivery to mesenchymal stem cells with antibacterial activity. Biomaterials. 2016; 103:137–149.
[158] Peng LH, Niu J, Zhang CZ, et al. TAT conjugated cationic noble metal nanoparticles for gene delivery to epidermal stem cells. Biomaterials. 2014;35(21): 5605–5618.,
[159] Yi Y, Kim HJ, Mi P, et al. Targeted systemic delivery of siRNA to cervical cancer model using cyclic RGD-installed unimer polyion complex-assembled gold nanoparticles. J. Control. Release. 2016; 244:247–256.
[160] Kim HJ, Takemoto H, Yi Y, et al. Precise engineering of siRNA delivery vehicles to tumors using polyion complexes and gold nanoparticles. ACS Nano. 2014; 8(9):8979–8991.
[161] Gong NQ, Teng XC, Li JH, et al. Antisense oligonucleotide-conjugated nanostructure-targeting lncRNA MALAT1 inhibits cancer metastasis. ACS Appl Mater Interfaces. 2019;11(1):37–42.
[162] Niu J, Chu Y, Huang YF, et al. Transdermal gene delivery by functional peptide-conjugated cationic gold nanoparticle reverses the progression and metastasis of cutaneous melanoma. ACS Appl Mater Interfaces. 2017;9(11):9388–9401.
[163] Huschka R, Barhoumi A, Liu Q, et al. Gene Silencing by gold nanoshell-mediated delivery and laser-triggered release of antisense oligonucleotide and siRNA. ACS Nano. 2012;6(9):7681–7691.
[164] French GL. Clinical impact and relevance of antibiotic resistance. Adv Drug Deliver Rev. 2005;57(10): 1514–1527.
[165] Hancock REW, Sahl HG. Antimicrobial and host-defense peptides as new anti-infective therapeutic strategies. Nat Biotechnol. 2006;24(12):1551–1557.
[166] Maleki H, Rai A, Pinto S, et al. High Antimicrobial activity and low human cell cytotoxicity of core-shell magnetic nanoparticles functionalized with an antimicrobial peptide. ACS Appl Mater Interfaces. 2016; 8(18):11366–11378.
[167] Casciaro B, Moros M, Rivera-Fernandez S, et al. Gold-nanoparticles coated with the antimicrobial peptide esculentin-1a(1-21)NH2 as a reliable strategy for anti-pseudomonal drugs. Acta Biomater. 2017; 47: 170–181.
[168] Yeom JH, Lee B, Kim D, et al. Gold nanoparticle-DNA aptamer conjugate-assisted delivery of antimicrobial peptide effectively eliminates intracellular *Salmonella enterica* serovar Typhimurium. Biomaterials. 2016; 104:43–51.
[169] Chen WY, Chang HY, Lu JK, et al. Self-assembly of antimicrobial peptides on gold nanodots: against multidrug-resistant bacteria and wound-healing application. Adv Funct Mater. 2015;25(46):7189–7199.
[170] Fan DX, Yao C, Zhou WY, et al. Ultrashort lipopeptides self-assembled with gold nanoparticles as potent antimicrobial agents. J Nanosci Nanotechnol. 2018; 18(12):8124–8132.
[171] Rai A, Pinto S, Evangelista MB, et al. High-density antimicrobial peptide coating with broad activity and low cytotoxicity against human cells. Acta Biomater. 2016; 33:64–77.
[172] Querido MM, Felgueiras HP, Rai A, et al. Cecropin-melittin functionalized polyurethane surfaces prevent staphylococcus epidermidis adhesion without inducing platelet adhesion and activation. Adv Mater Interfaces. 2018;5(24):1801390.
[173] White AD, Nowinski AK, Huang WJ, et al. Decoding nonspecific interactions from nature. Chem Sci. 2012; 3(12):3488–3494.
[174] Chen SF, Cao ZQ, Jiang SY. Ultra-low fouling peptide surfaces derived from natural amino acids. Biomaterials. 2009;30(29):5892–5896.
[175] Nowinski AK, White AD, Keefe AJ, et al. Biologically Inspired Stealth Peptide-Capped Gold Nanoparticles. Langmuir. 2014;30(7):1864–1870.

[176] Nowinski AK, Sun F, White AD, et al. Sequence, structure, and function of peptide self-assembled monolayers. J Am Chem Soc. 2012;134(13): 6000–6005.
[177] Wu JN, Lin Y, Li H, et al. Zwitterionic stealth peptide-capped 5-aminolevulinic acid prodrug nanoparticles for targeted photodynamic therapy. J Colloid Interface Sci. 2017;485:251–259.
[178] Wu JN, Han HJ, Jin Q, et al. Design and proof of programmed 5-aminolevulinic acid prodrug nanocarriers for targeted photodynamic cancer therapy. ACS Appl Mater Interfaces. 2017;9(17):14596–14605.